NAYARA PAULA ANDRADE VIEIRA

LASH MODEL USING HYDROLOGICAL RESPONSE UNITS (HRU) FOR SIMULATION OF THE CLIMATE CHANGE IMPACTS ON THE HYDROLOGY OF THE UPPER-MIDDLE GRANDE RIVER BASIN, SOUTHEAST BRAZIL

LAVRAS – MG
2019

NAYARA PAULA ANDRADE VIEIRA

LASH MODEL USING HYDROLOGICAL RESPONSE UNITS (HRU) FOR SIMULATION OF THE CLIMATE CHANGE IMPACTS ON THE HYDROLOGY OF THE UPPER-MIDDLE GRANDE RIVER BASIN, SOUTHEAST BRAZIL

Tese apresentada à Universidade Federal de Lavras, como parte das exigências do Programa de Pós-Graduação em Recursos Hídricos em Sistemas Agrícolas, para obtenção do título de Doutor.

Prof. Dr. Carlos Rogério de Mello
Orientador

Prof. Dr. Marcelo Ribeiro Viola
Coorientador

LAVRAS – MG
2019

Ficha catalográfica elaborada pelo Sistema de Geração de Ficha Catalográfica da Biblioteca Universitária da UFLA, com dados informados pelo(a) próprio(a) autor(a).

Vieira, Nayara Paula Andrade.

LASH model using hydrological response units (HRU) for simulation of the climate change impacts on the hydrology of the Upper-Middle Grande river basin, Southeast Brazil / Nayara Paula Andrade Vieira. - 2019.

106 p. : il.

Orientador(a): Carlos Rogério de Mello.

Coorientador(a): Marcelo Ribeiro Viola.

Tese (doutorado) - Universidade Federal de Lavras, 2019.

Bibliografia.

1. Simulação hidrológica. 2. Modelo LASH. 3. Mudanças climáticas. 4. Potencial hidroelétrico. I. Mello, Carlos Rogério de. II. Viola, Marcelo Ribeiro. III. Título.

NAYARA PAULA ANDRADE VIEIRA

LASH MODEL USING HYDROLOGICAL RESPONSE UNITS (HRU) FOR SIMULATION OF THE CLIMATE CHANGE IMPACTS ON THE HYDROLOGY OF THE UPPER-MIDDLE GRANDE RIVER BASIN, SOUTHEAST BRAZIL

MODELO HIDROLÓGICO LASH USANDO UNIDADES DE RESPOSTA HIDROLÓGICA (HRU) PARA SIMULAÇÃO DE IMPACTOS DAS MUDANÇAS CLIMÁTICAS NA HIDROLOGIA DA BACIA DO ALTO-MÉDIO RIO GRANDE, SUDESTE DO BRASIL

Tese apresentada à Universidade Federal de Lavras, como parte das exigências do Programa de Pós-Graduação em Recursos Hídricos em Sistemas Agrícolas, para obtenção do título de Doutor.

APROVADA em 17 de setembro de 2019
Dra. Tamara Leitzke Caldeira UFPEL
Dr. Junior Cesar Avanzi UFLA
Dr. Samuel Beskow UFPEL

Prof. Dr. Carlos Rogério de Mello
Orientador

Prof. Dr. Marcelo Ribeiro Viola
Coorientador

LAVRAS – MG
2019

“Entrega o teu caminho ao senhor, confia nele; e Ele tudo fará.”

A Deus,
Aos meus pais Jorge e Iara,
Aos meus irmãos Maykon e Nayane,
Ao meu namorado Douglas,

DEDICO

AGRADECIMENTOS

A Deus, razão da minha vida, por ter me dado força para superar os desafios e graça nos momentos de tribulação.

Aos meus pais, Jorge e Iara, e meus irmão, Maykon e Nayane, que não mediram esforços para a concretização dos meus sonhos, pelo amor incondicional, carinho, confiança e pelas orações.

Ao meu namorado, Douglas, pela dedicação, apoio, incentivo, amor e carinho. Por sempre acreditar que eu era capaz de superar os desafios encontrados nessa jornada.

As minhas tias Consuelo, Denise pelas orações.

A toda família, em especial a minha avó Olinta, pela torcida.

Ao meu orientador Carlos Rogério de Mello pelo conhecimento transmitido, pela orientação, apoio, paciência e pela confiança depositada em mim para a conclusão desse trabalho.

Ao coorientador Marcelo Ribeiro Viola por toda ajuda, ensinamentos e sugestões para realização desse trabalho.

As amigas lavrenses, Aline, Ingrid, Sarah Talita e Sara Ribeiro pela grande amizade, ajuda, orações e companheirismo.

Aos meus queridos amigos pelo companheirismo, pela amizade, que mesmo de longe sempre me acompanharam.

Aos meus sogros, Cleuza e Nilton, e meus cunhados, pelo carinho e torcida.

A todos os amigos, funcionários e professores do núcleo didático-científico de Engenharia de Água e Solo da UFLA, pela convivência, troca de experiências e companheirismo, em especial: Sany, Jéssica, Eduardo, Samuel, Vinicius, Brenon, Jacineumo e Ewerton.

Aos membros da banca, professores Junior César Avanzi, Samuel Beskow e Tamara Leitzke Caldeira pelas sugestões.

À Universidade Federal de Lavras e ao Programa de Pós-Graduação em Recursos Hídricos em Sistemas Agrícolas pela oportunidade de realização do curso.

À Coordenação de Aperfeiçoamento de Pessoal de Nível Superior (CAPES), pela concessão da bolsa de doutorado.

À Dra. Sin Chan Chou e sua equipe de pesquisa do CPTEC/INPE, por cederem os resultados das simulações dos modelos climáticos regionais utilizados nesse trabalho.

A todos aqueles que, direta ou indiretamente, participaram da realização deste trabalho.

MUITO OBRIGADA!

RESUMO GERAL

No Brasil, aproximadamente 70% de toda energia elétrica é produzida por usinas hidrelétricas (UHEs), tornando o país dependente do regime hidrológico. Assim, a capacidade de geração de energia elétrica no país pode ser comprometida em função das alterações no regime hidrológico, em especial, devido às mudanças climáticas. Nesse sentido, a modelagem do comportamento hidrológico de bacias hidrográficas representa uma importante ferramenta para a gestão dos recursos hídricos, sendo usada na avaliação de impactos, especialmente associados às mudanças climáticas. O objetivo desse estudo foi: i) aprimorar a estrutura do modelo Lavras Simulation of Hydrology (LASH) com a inserção do conceito de Unidades de Respostas Hidrológicas (HRUs) a fim de potencializar sua capacidade de simular o escoamento superficial e também o armazenamento de água no solo; ii) aplicar o modelo na simulação dos impactos climáticos nas condições hidrológicas e no potencial de geração de energia elétrica da usina hidrelétrica de Furnas (UHE-Furnas). O modelo foi calibrado e validado usando essa nova abordagem para a bacia hidrográfica do rio Grande, com seção definida na UHE-Furnas. Foram confeccionados mapas de armazenamento de água no solo para cada sub-bacia discretizada pelo modelo. Para simular os potenciais impactos nas condições hidrológicas devido às mudanças climáticas, considerou-se as premissas dos "Representative Concentration Pathways" (RCPs) 4.5 e 8.5 simuladas pelos modelos climáticos regionais (MCRs) Eta-HadGEM-ES, Eta-MIROC5 e Eta-CanESM2, entre os anos 2007 e 2099. A produção potencial anual média de energia elétrica pela UHE-Furnas foi estimada por meio das Curvas de Permanência de Energia (CPEs). Os resultados do coeficiente estatístico de Nash-Sutcliffe (C_{NS}), com passo diário, foram de 0,86 e 0,77, para as etapas de calibração e validação, qualificando o modelo como de alta performance para a simulação. O armazenamento de água no solo mostrou-se condizente com suas respectivas características geomorfológicas, climáticas e de uso do solo. Os resultados relacionados aos impactos hidrológicos de mudanças climáticas indicam redução da vazão média mensal durante todo o período analisado, independentemente do modelo climático (Eta-HadGEM2-ES, Eta-MIROC5 e Eta-CanESM2) e para ambos os cenários (RCP 4.5 e 8.5), com projeções mais críticas associadas ao modelo Eta-HadGEM2-ES. Estes resultados poderão levar a reduções no potencial hidrelétrico da UHE-Furnas de até -53% ao longo do século XXI.

Palavras-chave: Simulação hidrológica. Modelo LASH. Mudanças climáticas. Potencial hidroelétrico.

GENERAL ABSTRACT

In Brazil, approximately 70% of all electricity is produced through hydropower plants (HPs), which makes the country dependent on the hydrological regime. Therefore, the power generation capacity can be compromised due to climate change and its impacts over the hydrological regime. In this sense, the hydrological modeling represents an important tool in the context of water resources management. It can be used in the assessment of the impacts, especially associated with climate change. In this context, this study aims: i) to enhance the structure of Lavras Simulation of Hydrology (LASH) with the introduction of the concept of hydrological responses units (HRUs), which has potential to increase the ability of this model to simulate runoff and other hydrological variables, such as soil water storage; ii) to apply this improved version of the model to simulate the impacts on the hydrological conditions and the potential for electric energy generation of the Furnas hydroelectric plant (FHP). LASH model was calibrated and validated using this new approach for the Grande river basin defined at FHP. Soil water storage maps were developed made for each sub-basin discretized by the model. For simulation of the hydrological impacts from climate change, it was considered the Representative Concentration Pathways (RCPs) 4.5 and 8.5 premises simulated by the regional climate models (RCMs) Eta-HadGEM-ES, Eta-MIROC5 and Eta-CanESM2, between the years 2007 and 2099. The hypothetical average annual energy production for FHP was estimated through the Power Duration Curves (PDCs). The results of the Nash-Sutcliffe statistical coefficient (NS), in a daily step, were 0.86 and 0.77, respectively, for the calibration and validation, which allow qualifying the model as high performance for hydrological simulation. Soil water storage behavior was consistent with the geomorphological, climatic and land use characteristics. The results related to the hydrological impacts from climate change indicate a reduction in the monthly average streamflow over the analyzed period for all the RCM (Eta-HadGEM2-ES, Eta-MIROC5 and Eta-CanESM2) and RCPs. The more critical projections were those based on the Eta-HadGEM2-ES model, which resulted in a decrease in the annual energy production of up to -53% over the 21st century in FHP.

Keywords: Hydrological simulation. LASH model. Climate changes. Hydroelectric potential.

SUMÁRIO

PRIMEIRA PARTE

1 INTRODUÇÃO

A água é o recurso natural fundamental e sua disponibilidade está ligada, diretamente, às características da superfície terrestre, às condições climáticas, e ao consumo para diversas finalidades. Segundo Viola et al. (2013) a variabilidade do regime hidrológico é uma das principais caraterísticas dos ecossistemas tropicais e entender essa dinâmica e modelá-la sob o ponto de vista físico constituem importantes demandas da ciência ambiental.

O Brasil é um país extremamente dependente dos recursos hídricos. É considerado úmido em grande parte do seu território. Possui grandes rios, cuja importância está fortemente associada à geração de energia elétrica, e sua matriz hidráulica é responsável pela maior parte da energia consumida (NÓBREGA et al., 2011). Na bacia hidrográfica do rio Paraná, um complexo de usinas hidrelétricas de grande relevância energética para o Brasil está instalado, dentre eles a Usina hidrelétrica de Furnas – UHE Furnas.

A UHE Furnas localiza-se no alto-médio rio Grande, um dos principais afluentes do rio Paraná. Esta usina, além de gerar uma grande quantidade de energia, possibilita a regularização da vazão na bacia do Grande, promovendo reflexos diretos nos deflúvios superficiais da bacia do rio Paraná (FURNAS, 2007). Neste contexto, mudanças climáticas que afetem o alto-médio rio Grande, refletem em impactos não só em Furnas, mas em todo complexo de geração hidrelétrica instalado a jusante.

Estudos com base científica referentes às mudanças climáticas e à disponibilidade hídrica tomaram grande proporção nas últimas décadas, uma vez que os processos hidrológicos em bacias hidrográficas são muito sensíveis às

mudanças dos padrões de temperatura, precipitação e variações na concentração atmosférica dos gases do efeito estufa (ALVARENGA et al., 2016; TAN et al., 2017; ZHANG et al., 2016). Tais alterações climáticas afetam todos os componentes do ciclo hidrológico. Assim várias regiões do planeta sofrerão com a ocorrência de eventos extremos, como aumento na frequência de cheias, estresse hídrico de espécies vegetais, períodos de estiagem prolongados, entre outros (OLIVEIRA et al., 2017).

Diante desse cenário, foi estruturado o Painel Intergovernamental sobre Mudanças Climáticas (IPCC) pela Organização Meteorológica Mundial – OMM e pelo Programa das Nações Unidas para o Meio Ambiente – PNUMA em 1998. O IPCC tem como objetivo principal fornecer informações científicas para melhorar o entendimento sobre mudanças no clima global, visto que são projetadas alterações nos regimes térmico e pluvial com consequências diretas no ciclo hidrológico, trazendo reflexos na capacidade de produção de água das bacias, especialmente nas regiões tropicais e subtropicais.

Visando à modelagem do comportamento hidrológico de bacias hidrográficas, os modelos hidrológicos têm sido amplamente explorados. A simulação hidrológica tem se consolidado no âmbito científico graças à interação entre os modelos hidrológicos, os Sistemas de Informações Geográficas (SIGs) e as técnicas de sensoriamento remoto. Segundo Green et al. (2006) essa importante ferramenta no contexto de gestão dos recursos hídricos, vem sendo usada na avaliação de impactos hidrológicos de uma bacia hidrográfica, especialmente associados a mudanças climáticas e no uso do solo.

Nesse âmbito, estudos que buscam associar modelos hidrológicos aos modelos climáticos estão sendo amplamente utilizados. Dentre os vários modelos hidrológicos desenvolvidos, destaca-se o modelo Lavras Simulation of Hydrology (LASH) originalmente elaborado por Mello et al. (2008). O LASH vem sendo aprimorado desde então e tem sido aplicado a diferentes bacias hidrográficas de

Minas Gerais, Tocantins e Rio Grande do Sul, com resultados promissores no tocante à sua acurácia, e com pequeno número de parâmetros a serem calibrados (BESKOW; NORTON; MELLO, 2013; CALDEIRA et al., 2019; VIOLA, 2008; VIOLA et al., 2014, 2015). O LASH encontra-se atualmente na sua terceira versão, no entanto o conceito de Unidades de Resposta Hidrológica (HRUs) não foi testado no LASH. De acordo com Neitsch et al. (2005) seu conceito é embasado na classificação hidrológica de diferentes áreas de uma bacia que apresentem a mesma combinação de relevo, solos e usos do solo, independentemente da sua localização geográfica.

Diante do exposto, este estudo foi realizado com os objetivos de: (i) inserir o conceito de Unidades de Respostas Hidrológicas (HRUs) na estrutura atual do modelo LASH com o intuito de aperfeiçoar sua calibração e validação na escala diária; (ii) utilizar essa nova abordagem na calibração e validação do modelo para simular o escoamento, bem como o armazenamento de água no solo, na bacia hidrográfica do rio Grande, com seção definida na Usina Hidrelétrica de Furnas; iii) simular os impactos hidrológicos decorrentes de mudanças climáticas simuladas pelos modelos climáticos regionais Eta-HadGEM2-ES, Eta-MIROC5 e Eta-CanESM2, associadas aos Cenários Representativos de Concentração RCP 4.5 e RCP 8.5, ao longo do século XXI; e iv) simular os impactos no potencial de produção de energia elétrica na usina hidrelétrica de Furnas proporcionados pelas mudanças climáticas.

2 REFERENCIAL TEÓRICO

2.1 Modelagem hidrológica

A modelagem hidrológica é essencial para análise e interpretação dos fenômenos envolvidos no ciclo hidrológico devido às complexas relações entre os componentes desse ciclo. Os modelos hidrológicos são uma representação simplificada do sistema real a ser estudado. Dessa forma, um modelo hidrológico pode ser entendido como uma representação dos fenômenos associados ao ciclo hidrológico nas bacias hidrográficas, o qual simula os processos naturais em função dos estímulos físicos e climáticos (SOROOSHIAN et al., 2008).

2.1.1 Classificação dos modelos hidrológicos

As classificações aplicadas a modelos hidrológicos englobam diferentes aspectos relacionados à sua estrutura, objetivos, discretização do tempo e no espaço, entre outros. De acordo com Rennó e Soares (2000), modelos hidrológicos podem ser classificados com base nas variáveis utilizadas na modelagem, nas relações entre essas variáveis, a forma de representação dos dados no tempo e no espaço e a existência ou não de relações.

Segundo Shaw (1994), os modelos que consideram o conceito de probabilidade em seu equacionamento podem ser classificados como estocásticos ou determinísticos. O modelo estocástico baseia-se nas leis da probabilidade, a fim de gerar séries hidrológicas, enquanto o determinístico procura simular os processos físicos envolvidos na transformação da precipitação em escoamento superficial (RENNÓ, 2003; TUCCI, 2005).

Quanto ao tipo de formulação envolvida os modelos podem ser empíricos, físicos, conceituais ou semi-conceituais. Os modelos empíricos utilizam relações fundamentadas em observações, as quais são frequentemente realizadas por funções estatísticas que não têm qualquer relação com os processos físicos envolvidos (SILVA; TUCCI; COLLISCHONN, 2006). Viola (2011) relata que os modelos físicos fazem o uso das principais equações diferenciais encontradas no

sistema do mundo real para representar os processos, e seus parâmetros são os mais semelhantes possíveis à realidade física. Os modelos semi-conceituais seguem a premissa da relação com as leis que regem os fenômenos, contudo, ainda possuem algum grau de empirismo uma vez que são empregados parâmetros calibráveis (DURÃES, 2010).

Os modelos classificados quanto à forma de representação dos dados no tempo, podem ser contínuos ou discretos. Quando os fenômenos são representados continuamente no tempo, objetivando a modelagem por longos períodos, são entendidos como contínuos; quando as variáveis são obtidas por períodos isolados de uma série histórica, buscando representar eventos de cheia ou recessão, são do tipo discretos (MARINHO FILHO et al., 2012; PEREIRA, 2013).

Quanto à forma de representação espacial, os modelos são classificados em concentrados ou distribuídos. Em modelos concentrados considera-se que todas as variáveis de entrada e de saída são representativas de toda área estudada, o que limita a representação da variabilidade espacial das características da bacia, dada sua natural heterogeneidade (HARTMANN; BALES; SOROOSHIAN, 1999; VIOLA, 2011). Em contrapartida, os modelos distribuídos consideram a variabilidade espacial encontrada nas diversas variáveis do modelo (SILVA TUCCI; COLLISCHONN, 2006). Dessa forma a bacia hidrográfica ser subdividida em sub-bacias ou em células, proporcionando melhor descrição da variabilidade espacial dos processos e das variáveis de entrada (COLLISCHONN; TUCCI, 2001). De acordo com Arnold et al. (1998) e Gassman et al. (2007) existem modelos, como por exemplo o SWAT, no qual as sub-bacias são divididas em Unidades de Resposta Hidrológica (HRUs). Seu conceito é embasado na classificação hidrológica de diferentes áreas de uma bacia que apresentem a mesma combinação de relevo, solos e usos do solo, independentemente da sua

localização geográfica, sendo consideradas unidades hidrologicamente homogenias (NEITSCH et al., 2005).

2.1.1 Desempenho de modelos hidrológicos

São vários os modelos disponíveis para simulação hidrológica. A partir dessa grande disponibilidade de modelos hidrológicos diversos estudos têm sido realizados, com o intuito de quantificar os efeitos das alterações no uso e cobertura do solo sobre a dinâmica do escoamento em bacias hidrográficas e dos impactos de mudanças climáticas no ciclo hidrológico.

Em um estudo conduzido na região Alto Rio Grande, sul de Minas Gerais, Mello et al. (2008) aplicaram a primeira versão do modelo LASH, distribuída por sub-bacias, para avaliar os impactos hidrológicos decorrentes da substituição de pastagens por eucalipto. Os autores verificaram uma tendência de redução no escoamento da ordem de 105 mm ano^{-1}, após a modificação de 28,2% da cobertura vegetal.

Durães, Mello e Naghettini (2011) usaram o modelo SWAT para simular o comportamento hidrológico da bacia do rio Paraopeba – MG sob diferentes usos e ocupação do solo e encontraram resultados satisfatórios, atingindo um coeficiente de Nash-Sutcliffe superior a 0,75. Andrade, Mello e Beskow (2013), com o objetivo de calibrar e validar o modelo SWAT para simulação do escoamento superficial na bacia hidrográfica do Ribeirão Jaraguara – MG, obteve uma acurácia do modelo, com base no coeficiente de Nash-Sutcliffe, de 0,66 e 0,87 para as fases de calibração e validação respectivamente.

Avaliando a aplicabilidade do modelo LASH para simulação hidrológica das bacias hidrográficas que compõem a cabeceira da bacia do rio Grande (sul de Minas Gerais), Viola et al. (2013) verificaram que o modelo simulou, de forma adequada, o regime hidrológico das bacias, apresentando coeficiente de Nash-

Sutcliffe superior a 0,70. Viola et al. (2014) realizaram um estudo para avaliar os impactos das mudanças do uso da terra na hidrologia das bacias de cabeira do rio Grande e concluíram que alterações no uso da terra podem fazer com que as bacias fiquem mais propensas a inundações e outros riscos associados com o aumento do escoamento superficial.

2.2 Mudanças Climáticas

O sistema climático integra cinco componentes principais que se relacionam entre si: a atmosfera, a hidrosfera, a criosfera, a litosfera, e a biosfera. Por influência da própria dinâmica da terra e devido às forçantes externas naturais e antropogênicas, esse sistema modifica-se com o passar do tempo. Quando as variações permanecem constantes, a um nível de probabilidade significativo e perdurando por um longo período (décadas ou mais) nesse sistema, evidencia-se uma mudança climática (IPPC, 2013).

Com a intensificação das mudanças climáticas e das atividades antropogênicas, acredita-se que o ciclo hidrológico global está alterando de forma significativa (IPPC, 2013). A intensidade e as características dessas alterações climáticas podem variar significativamente de uma região para outra. Sun et al. (2014) exemplificam que algumas regiões do globo terrestre podem enfrentar secas severas, enquanto outras podem sofrer com inundações.

As alterações que ocorrem na temperatura global estão interligadas diretamente a modificações no balanço entre entrada e saída e energia no planeta que, por sua vez, sofre com a atuação de fatores como a quantidade de “gases de efeito estufa – GEE” e aerossóis na atmosfera, radiação solar, propriedades da superfície terrestre, entre outros. Tais fatores representam perturbações impostas ao sistema climático, e podem ser de origem natural ou humana (NEELING,

2011). A percepção de sua influência sobre o aquecimento ou o resfriamento do clima global, geralmente é expressa por meio de um índice, chamado forçamento radiativo, expresso em watts por metro quadrado (W m^{-2}) (IPCC, 2007; 2013).

A sensibilidade climática é outra forma empregada para avaliar a resposta climática à forçantes radiativas. Para o IPPC (2014), esse conceito representa a alteração do equilíbrio na média global anual da temperatura do ar superficial após uma duplicação no equivalente de CO_2 atmosférico, ou seja, representa quanto a temperatura aumenta quando a quantidade de CO_2 duplica.

Segundo Barry e Chorley (2013), a duplicação na concentração de CO_2 equivale a uma forçante radiativa de aproximadamente 4 W m^{-2}. O equilíbrio radiativo seria restaurado novamente, com uma temperatura superficial nova e mais alta após determinado ponto. Predições da sensibilidade climática obtidas com a geração de modelos climáticos globais e atuais variam de 2,1 a 4,4 °C, com a melhor estimativa em 3.0 °C (FORSTER et al., 2013).

No documento publicado pelo Painel intergovernamental de Mudanças Climáticas (IPCC, 2013) são apresentados modelos de projeções climáticas que indicam que sob um cenário mais pessimista, a temperatura da superfície da Terra poderá aumentar de 1,1 a 6,4 ºC durante o século XXI.

Segundo Adam e Collischonn (2013), mesmo que grande parte da comunidade científica aceite as evidências de que a maior parte do aquecimento global nos últimos anos é uma resposta ao aumento nas concentrações de GEE na atmosfera, ainda existem lacunas associadas ao tema, causando opiniões contraditórias. Mas, recentemente, o estudo realizado por Neukom et al. (2019) demonstrou que essa especulação não é mais válida. O artigo traz evidências de que o período mais quente dos últimos dois milênios ocorreu durante o século XX, em mais de 98% do planeta, reafirmando o aquecimento global.

2.3 Modelos Climáticos

Para investigar a resposta do sistema climático, os modelos climáticos são as principais ferramentas disponíveis. Estes modelos fazem simulações do clima em diferentes escalas de tempo, e, por conseguinte, projeções de futuras alterações climáticas (IPCC, 2013). Nos Modelos de Circulação Geral (MCG's), conhecidos como modelos climáticos globais, o sistema climático é descrito em termos do comportamento físico, químico e biológico da atmosfera, modelados com equações que expressam essas leis (MARENGO et al., 2012).

Segundo o IPCC (2013) a escolha do modelo depende diretamente da questão científica a ser abordada, uma vez que os MCG's vão desde modelos simples de equilíbrio de energia a modelos mais complexos que requerem alto desempenho computacional.

Apesar dos diferentes MCG's constituírem as ferramentas padrão para melhor compreensão das potenciais alterações no sistema climático sua resolução é espacialmente grosseira, o que limita a simulação climática dos processos de mesoescala, especialmente na representação da topografia e uso do solo (BROWN et al., 2014).

Para se alcançar uma melhor resolução espacial das mudanças climáticas, em nível regional, métodos de regionalização, conhecidos como downscaling, têm sido desenvolvidos (BARDOSSY; PEGRAN, 2012; FOWLER; BLENKINSOP; TEBALDI, 2007; TEUTSCHBEIN; WETTENHALL; SEITBERT, 2011). Esse termo se refere às técnicas de transferência de informação climatológica derivada dos MCG's, geralmente com resolução maior que 100 km, para as escalas regionais, compatíveis com bacias hidrográficas, especialmente de médio e grande portes (BARDOSSY; PEGRAN, 2012; FOWLER; BLENKINSOP; TEBALDI, 2007).

Modelos Climáticos Regionais (MCR's) permitem a aplicação dos cenários de mudanças climáticas em pequenas e médias bacias por possuírem resolução espacial entre 5 e 50 km (MARENGO et al., 2009; 2012). Os MCR's incorporam características regionais como topografia, vegetação, solo e outras, não contidas ou simplificadas pelos modelos globais (CHOW et al., 2014). A utilização conjunta dos MCR's possibilita o detalhamento espacial dos processos climáticos a nível local ou regional, detectando as variações e particularidades de uma determinada região, o que melhora a compreensão de impactos em bacias hidrográficas (MARENGO et al., 2010, 2012).

Kawazoe e Gutowski (2013) e Vautard et al. (2013) salientam que apesar das incertezas envolvendo o processo de modelagem atmosférica e projeções climáticas, vários estudos usando modelos climáticos regionais sugerem melhor desempenho nos resultados obtidos em comparação aos MCG's. No Brasil, o Centro de Previsão de Tempo e Estudos Climáticos (CPTEC) do Instituto Nacional de Pesquisas Espaciais (INPE) vem trabalhando com modelos regionalizados, como, por exemplo, o Modelo Regional ETA/CPTEC, com resoluções de até 5 km (MOURÃO; CHOU; MARENGO, 2016). De acordo com Chou (1996), o modelo regional Eta tem como propósito prever com maior precisão fenômenos associados a frentes, orografia, brisa marítima, tempestades severas, etc., ou seja, sistemas organizados em mesoescala. Dessa forma, o Eta produz a regionalização das simulações dos MCGs sobre a América do Sul e a América Central.

Pesquisas que utilizaram MCR's para o estudo das mudanças climáticas na América do Sul podem ser observadas em Garreaud e Falvey (2008); Marengo et al. (2010); Menéndez et al. (2010); Nuñez, Solman e Cabré (2008); Rocha et al. (2009); Soares e Marengo (2009); Solman, Nuñez e Cabré (2008).

2.4 Impactos decorrentes de mudanças climáticas

As mudanças climáticas causam uma grande alteração na disponibilidade dos recursos hídricos. Algumas das principais consequências dessa mudança são o aumento da variabilidade da precipitação, maior ocorrência e magnitude de eventos extremos, como secas prolongadas, cheias e mudança na frequência de vazões (BELL et al., 2007; HAGUMA et al., 2014).

Com a finalidade, avaliar os impactos hidrológicos decorrentes dessas mudanças climáticas, muitos estudos têm sido empregado como variáveis de entrada em modelos hidrológicos, dados simulados a partir da saída de MCG's ou de MCR's, obtendo importantes resultados para a gestão de recursos hídricos.

Ouyang et al. (2015) utilizaram seis modelos climáticos globais (MCG's) sob a influência dos cenários RCPs 2.6, 4.5 e 8.5, acoplados ao modelo SWAT, para avaliar o impacto das mudanças climáticas na bacia hidrográfica Huangzhunang, na China. Os modelos projetaram, em média, uma variação da precipitação entre a metade e no final do século XXI, de 2,4% a -9%. Entretanto as previsões indicaram uma redução na vazão, variando de 6,9% a 0,8% devido, principalmente, ao aumento da evapotranspiração na bacia em estudo.

No estudo realizado na bacia do rio Lhasa, no planalto do Tibete, Liu et al. (2015) investigaram os plausíveis regimes hidrológicos futuros, pelo método downscaling, a partir de dois MCG's (Echam5 e Miroc3.2_Medres), sobre três cenários (A1B, A2 e B1) para o período de 2046-2065. Os resultados mostraram aumento da temperatura do ar e da precipitação anual. A temperatura máxima do ar pode ter um aumento maior que 2ºC, ao passo que a precipitação anual poderá ter um ligeiro aumento. A variação na precipitação mensal será mais significativa, com um aumento acentuado no verão e reduções drásticas nas demais. A evaporação e a vazão terão uma tendência de crescimento, enquanto que a

cobertura da neve reduzirá drasticamente. Os autores salientam que os resultados devem ser utilizados como referência para a gestão dos recursos hídricos nessas regiões vulneráveis.

Guo et al. (2016) avaliaram os impactos das alterações climáticas na bacia do rio Xiying, no noroeste da China, utilizando o modelo HadCM3 para os cenários SRES A2 e B2 acoplados ao modelo hidrológico SWAT. Os resultados indicaram que a vazão média anual poderá diminuir em 5,4% e 4,5% para os cenários A2 e B2, respectivamente, para o período de 2010 a 2039. Enquanto que para o período de 2040-2069 as projeções indicam reduções de 21,2% e 16,9% na vazão anual, para os mesmos cenários, respectivamente.

Tan et al. (2017), utilizando o modelo hidrológico SWAT, avaliaram os possíveis impactos decorrentes de mudanças climáticas na bacia hidrográfica do rio Kelantan, na Malásia, associado aos cenários RCPs 2.6, 4.5 e 8.5 projetado por 5 MCGs, nos períodos de 2015-2044 e 2045-2074. Os resultados indicaram aumentos médios nas vazões para os três RCPs de 14,6 e 27,2%, nos períodos de 2015-2044 e 2015-2074, respectivamente, com aumentos mais significativos no cenário RCP 8.5.

No Brasil, Viola et al. (2015) simularam os impactos das possíveis mudanças climáticas no comportamento hidrológico na cabeceira da bacia do rio Grande, partir do modelo hidrológico LASH associado ao modelo climático Eta/HadCM3, para o cenário climático A1B nos períodos de 2011-2040, 2041-2070 e 2071-2098. Os resultados mostraram que poderá ocorrer uma redução do escoamento anual nas bacias analisadas, para o período de 2011-2040, mas para os demais períodos há uma tendência de aumento no escoamento anual.

Ho, Thompson e Brierley (2016) investigaram os possíveis impactos decorrentes de mudanças climáticas na bacia hidrográfica dos rios Tocantins-Araguaia no final do século 21 (2071-2100). Para alcançar os objetivos, os autores utilizaram um conjunto de 41 MCG’s sob influência do Cenário RCP 4.5

acoplados ao modelo hidrológico STELLA. Os resultados indicaram que a maioria dos modelos climáticos uma redução na vazão anual média apesar de alguns MCG's apresentarem aumento. Durante a transição entre o período seco e chuvoso, a maioria das simulações evidenciaram uma expressiva redução nas vazões. Além disso, 75% dos modelos analisados sugerem uma redução nas vazões mínimas, o que poderia prejudicar o planejamento atual e futuro da rede de produção de energia na bacia.

Alvarenga et al. (2016) simularam os impactos hidrológicos, decorrentes das mudanças climáticas, na bacia hidrográfica Lavrinha, localizada no Sul de Minas Gerais. Para alcançar os resultados os autores utilizaram o modelo hidrológico DHSVM forçado pelo modelo Eta/HadGEM2-ES, sob a influência do cenário RCP 8.5 ao longo do século XXI. As projeções indicaram reduções nas vazões médias mensais variando entre 20 e 77% ao longo do século XXI (2011 a 2099), correspondendo a reduções drásticas no escoamento.

2.5 Impactos na produção de energia elétrica

No Brasil, a produção de energia elétrica é composta por um sistema hidro-termo-eólico de grande porte, predominantemente com base em geração hídrica, distribuídas em diferentes bacias hidrográficas nas diferentes regiões do país (BUENO, 2018). Segundo a Agência Nacional de Energia Elétrica (ANEEL, 2017) o país possui 1.265 usinas hidrelétricas (UHEs), correspondendo a 70% da capacidade instalada de energia elétrica no país. Tal fato faz com que o Brasil ocupe o 3º lugar no ranking mundial de geração hidrelétrica, ficando atrás do Canadá e da China (INTERNATIONAL ENERGY AGENCY – IEA, 2017). Além disso, a energia elétrica produzida no país possui características únicas quando comparadas ao de outros países (EPE, 2013).

Em 2012, 77% (455,6TWh) da energia elétrica produzida proveio das UHEs, entretanto, devido à condições hidrológicas desfavoráveis, a participação da geração hídrica foi relativamente pequena (EPE, 2013). Em um ano mais próximo ao comportamento padrão a participação da hidroeletricidade na matriz elétrica brasileira pode chegar a 82%, como em 2011 e em 2016, quando a geração média foi de 73,4% (EPE, 2013; ONS, 2017).

De acordo com Zhao e Liu (2015), a hidroeletricidade é uma fonte de energia renovável e baixa emissão de gases de efeito estufa. No entanto, diante do cenário atual de mudanças climáticas e escassez dos recursos hídricos tornou-se importante e vital para sustentabilidade técnica, econômica e social o conhecimento mínimo sobre a hidrologia comportamental dos rios, avaliação de características hidráulicas e flutuações hidrometeorológicas (LIU et al., 2015; SOUZA et al., 2011). Eventos extremos de chuva, por exemplo, podem prejudicar ou comprometer a instalação e operação dos aproveitamentos hidrelétricos, que constituem o Sistema Interligado Nacional - SIN (SOUZA et al., 2011).

A abordagem metodológica amplamente aplicada para análise de impactos de mudanças climáticas na produção de energia consiste em estimar o escoamento por meio de modelos climáticos (MCG's ou MCR's) acoplados aos modelos hidrológicos (SCHAEFFER et al., 2012). De acordo com Majone et al. (2016), a análise de impactos no potencial de geração de energia elétrica fornece uma sólida medida indicativa de possíveis tendências na produção de energia relacionadas às mudanças climáticas.

Diante desse cenário, diversos estudos têm adotado esta metodologia com a finalidade de avaliar os impactos das mudanças climáticas no potencial de produção de energia no mundo, como pode ser observado na Tabela 1.

Tabela 1. Estudos que avaliaram impactos das mudanças climáticas no potencial de produção de energia elétrica em diversas regiões do mundo.

UHE	Bacia	MCG/ MCR	Modelo Hidrológico	Impacto	Autor (es)
5.991 UHEs europeias	Bacias europeias/Europa	HadCM3 ECHAM/OPY3	WaterGAP	▪ Redução no potencial anual de produção em mais de 25% no sul e centro-leste europeu (Espanha, Turquia, Bulgária e Ucrânia, especialmente). ▪ Aumento no potencial anual de produção em mais de 25% no norte europeu (Noruega, Finlândia, Suécia e Rússia, especialmente).	Lehner, Czisch e Vassolo (2005)
Chute-des-passes	Peribonka/Canadá	CRCM-CGCM3	Hydrotel	▪ Redução na produção anual de 1,8% no período de 2010 a 2039.	Minville et al. (2009)

Chute-du-diable Chute-a-la-savane				▪ Aumento na produção anual de 9,3% e 18% nos períodos de 2040-2069 e 2070-2099, respectivamente.	
Teles Pires	Tapajós/Brasil	8 MCGs	MDH-INPE	▪ Deixará de operar em 59% do tempo durante o período de 2041-2070. ▪ Redução de 82% na produção anual de energia.	Mohor et al. (2015)
Santo Antônio	Madeira/Brasil	8 MCGs	MDH-INPE	▪ Não houve consenso entre os modelos; ▪ Alguns apresentaram reduções de 45% e outros aumento de 38% de 2017 a 2099.	Siqueira Júnior, Tomasella e Rodriguez (2015)

24.515 UHEs	Ao redor do mundo	5 MCGs	VIC	▪ 74% da maioria das UHEs estão localizadas em regiões onde projeções de reduções significativas nas vazões são esperadas, resultando em reduções globais médias na capacidade utilizável da energia hidrelétrica. ▪ Reduções mensais na capacidade de produção de 9,2%, 17% e 24% para as décadas de 2020, 2050 e 2080, com 22% das usinas com reduções no potencial de geração maiores que 30% para a década de 2050.	Van Vliet et al. (2016)

5 UHEs	Noce/ Itália	5 MCRs: ECH-RCA ECH-REM ECH-RMO HCH-RCA	GEOTRANSF	▪ As maiores mudanças no potencial hidrelétrico serão nas maiores altitudes em função do aumento da precipitação. ▪ As mudanças nas produções de energia elétrica potencial variaram de -12,4% a + 213,4%	Majone et al. (2016)
Gabriel y Galan Buendía e Fratel	Targus/Portugal e Espanha	ISI-MIP	SWIM	▪ Redução no potencial de produção variado entre 10% e 50%, no RCP 4.5, para os períodos de 2021-2050 e 2071-2100, respectivamente. ▪ Redução no potencial de produção variado de 40 a 60%, no RCP 8.5, para os	Lobanova et al. (2016)

				períodos de 2021-2050 e 2071-2100, respectivamente.	
Ceppo Morelli	Anza/Alpes italianos	CCM-CM e 3 cenários definidos	Modelo conceitual semi-distribuido	▪ Redução no potencial de geração de energia hidrelétrica entre -40% e -19% em 2050 com relação ao período de referência.	Bongio, Avanzi e Michele (2016)
Camargos, Itutinga e Funil	Grande/ Brasil	Eta-HADGEM Eta-MIROC5	SWAT	▪ As usinas estudas poderão deixar de operar em 27,7%, 69,1% e 50%, do tempo, em Camargos, Itutinga e Funil considerando o modelo Eta-HadGEM ▪ A produção anual de energia pode reduzir em 57,2%, 66,1% e 38,2% em Camargos, Itutinga e Funil, entre 2071 e	Oliveira et al. (2017)

				2099 de acordo com o Eta-HADEM/RCP 8.5. ▪ O modelo Eta-MIROC5/RCP 4.5 indicou reduções na produção anual de energia 17,4%, 23,1% e 30,7% em Camargos, Itutinga e Funil, entre 2071 e 2099.	
Jubones	Jubones, Equador	Foram usados apenas 3 cenários de mudança de temperatura e precipitação	SWAT	▪ Usina enfrentará escassez de energia significativa, durante a estação seca, de até 13,14% em relação ao cenário de referência. ▪ A produção hidrelétrica anual será aumentada em 8%, como resultado do aumento de 13% na vazão no período chuvoso	Hasan e Wyseure (2018)

				devido a um aumento de 15% da precipitação.	
42 UHEs	42 bacias nos Alpes italianos dividas em 5 regiões: Piemonte, Valle d'aosta, Lambardia, Trentino, e Veneto	Não usaram MCG/MCR Os cenários foram definidos a partir de tendências observadas	Modelo conceitual semi-distribuido	▪ Redução de 3% na produção de energia elétrica até 2065 em todas as bacias.	Patro, Michele e Avanzi (2018)

CONSIDERAÇÕES GERAIS

Esta tese trabalhou no aprimoramento do modelo Lavras Simulation of Hydrology (LASH) para então aplicá-lo na simulação de impactos decorrentes de mudanças climáticas na bacia do rio Grande delimitada na Usina Hidrelétrica de Furnas (UHE-Furnas), bem como sua capacidade em simular o armazenamento de água no solo nas unidades hidrológicas consideradas na calibração do modelo. Dessa forma, pretende-se oferecer subsídios para uma melhor gestão de recursos hídricos na região. No aprimoramento do modelo LASH, foi inserido o conceito de Unidades de Respostas Hidrológicas (HRUs) na estrutura atual do modelo, com o intuito de aperfeiçoar sua calibração e validação, potencializando sua capacidade de prever os parâmetros do balanço hídrico.

Para a simulação climática foram utilizados três modelos climáticos regionais, Eta-HadGEM2-ES, Eta-MIROC5 e Eta-CanESM2, simulados sob influência de duas forçantes de concentração, RCP 4.5 e RCP 8.5. Consecutivamente, foram avaliados os impactos decorrentes dessas mudanças climáticas no potencial de geração de energia elétrica na usina hidrelétrica de Furnas, Alto-Médio rio Grande.

É importante ressaltar que este trabalho tem a finalidade de investigar e propor melhorias metodológicas para pesquisas futuras, complementando o estado da arte com relação à avaliação de impactos hidrológicos decorrentes de mudanças climáticas na produção de energia na bacia do rio Paraná.

REFERÊNCIAS

ADAM, K. N.; COLLISCHONN, W. Análise dos impactos de mudanças climáticas nos regimes de precipitação e vazão na bacia hidrográfica do rio Ibicuí. **Revista Brasileira de Recursos Hídricos**, Porto Alegre, v. 18, n. 3, p. 69-79, 2013.

ALVARENGA, L. A. et al. Hydrological responses to climate changes in a headwater watershed. **Ciência e Agrotecnologia**, Lavras, v. 40, n. 6, p. 647-657, 2016.

ANDRADE, M. A.; MELLO, C. R.; BESKOW, S. Simulação hidrológica em uma bacia hidrográfica representativa dos Latossolos na região Alto Rio Grande, MG. **Revista Brasileira de Engenharia Agrícola e Ambiental**, Campina Grande, v. 17, n. 1, p. 69-76, 2013.

AGÊNCIA NACIONAL DE ENERGIA ELÉTRICA. (Brasil). **Banco de Informações de Geração - BIG**. Brasília, 2017. Disponível em: <http://www 2.aneel.gov.br/aplicacoes/ capacidadebrasil/capacidadebrasil.cfm>. Acesso em: 20 jan. 2019.

BÁRDOSSY A, PEGRAM G. Multiscale spatial recorrelation of RCM precipitation to produce unbiased climate change scenarios over large areas and small. **Water Resources Research**, Washington, v. 48, n. 9, p. 1-13, 2012.

BARRY, R. G.; CHORLEY, R. J. **Atmosfera, Tempo e Clima**. 9 ed. Porto Alegre: Bookman, 2013. 512 p.

BELL, V. A. et al. Use of a grid-based hydrological model and regional climate model outputs to assess changing flood risk. **International Journal of Climatology**, Chichester, v. 27, n. 12, p. 1657–1671, 2007.

BESKOW, S.; NORTON, D. L.; MELLO, C. R. Hydrological prediction in a tropical watershed dominated by Oxisols using a distributed hydrological model. **Water Resources Management**, Reidel, v. 23, p. 341-363, 2013.

BONGIO, M.; AVANZI, F.; MICHELE, C. Hydroelectric power generation in an Alpine basin: future water-energy scenarios in a run-of-the-river plant. **Advances in Water Resources**, Oxford, v. 94, p. 318–331, May 2016.

BROWN, J. N. et al. Impact of projected climate change on hydrologic regime of the Upper Paraguay River basin. **Climatic Change**, Dordrecht, v. 127, p. 27-41, 2014. (DOI 10.1007/s10584-013-0816-2).

BUENO, E. O. Pegada hídrica das usinas hidrelétricas do Sistema Interligado Nacional na região hidrográfica do Paraná. 2018. 371p. **Tese** (Doutorado em Recursos Hídricos em Sistemas Agrícolas) Universidade Federal de Lavras, Lavras, 2018.

CALDEIRA. T. L. et al. LASH hydrological model: An analysis focused on spatial discretization. **Catena**, Amsterdam, v. 173, p. 183-193, 2019.

CHOU, S.C. **Modelo Regional Eta. Climanálise**. Edição Especial. Instituto Nacional de Pesquisas Espaciais. 1996.

CHOU, S. C. et al. Assessment of Climate Change over South America under RCP 4.5 and 8.5 Downscaling Scenarios. American **Journal of Climate Change**, Bethesda, v. 03, p. 512-527, 2014.

COLLISCHONN, W.; TUCCI, C. E. M. Simulação hidrológica de grandes bacias. **Revista Brasileira de Recursos Hídricos**, Porto Alegre, v. 6, n. 1, p. 95-118, 2001.

DURÃES, M. F. Caracterização e avaliação do estresse hidrológico da bacia do rio Paraopeba, por meio de simulação chuva-vazão de cenários atuais e prospectivos de ocupação e uso do solo utilizando um modelo hidrológico distribuído. 2010. 147 p. **Dissertação** (Mestrado em Saneamento, Meio Ambiente e Recursos Hídricos) - Universidade Federal de Minas Gerais, Belo Horizonte, 2010.

DURÃES, M. F.; MELLO, C. R.; NAGHETTINI, M. Applicability of the SWAT model for hydrologic simulation in Paraopeba River Basin, MG. **Cerne**, Lavras, v. 17, n. 4, p. 481-488, 2011.

EMPRESA DE PESQUISA ENERGÉTICA (EPE). **Balanço Energético Nacional 2013** – Ano base 2012: Relatório Síntese. EPE, Rio de Janeiro. 2013. Disponível em: <https://ben.epe.gov.br> Acesso em 15 de abril de 2018.

FORSTER, P. M. et al. Evaluating adjusted forcing and model spread for historical and future scenarios in the CMIP5 generation of climate models. **Journal of Geophysical Research**, v. 118, n. 3, p. 1139 – 1150, 2013.

FOWLER, H. J.; BLENKINSOP, S.; TEBALDI, C. Linking climate change modeling to impacts studies: recent advances in downscaling techniques for hydrological modeling. Int. **Journal of Climatology**, Chichester, v. 27, p. 1547-1578, 2007.

FURNAS. 1957-1967 – Como tudo começou. **Revista FURNAS**. Ed. especial, n. 337, fev. 2007. 17 p. Disponível em:

<http://www.furnas.com.br/arqtrab/ddppg/revistaonline/linhadireta/rf337_57-67.pdf>. Acesso em: 15 mai. 2019.

GARREAUD, R.; FALVEY, M. The coastal winds off western subtropical South America in future climate scenarios**. International Journal of Climatology**, Chichester, v. 29, p. 543–554. 2008.

GREEN, C. H. et al. Hydrologic evaluation of the soil and water assessment tool for a large tile-drained watershed in Iowa. **Transactions of the ASABE**, Saint Joseph, v. 49, n. 2, p. 413-422, 2006.

GUO, J. et al. Impacts of Climate and Land Use/Cover Change on Streamflow Using SWAT and a Separation Method for the Xiying River Basin in Northwestern China. **Water**, Basel, v. 8, n. 5, p. 1–14, 2016.

HAGUMA, D. et al. Optimal hydropower generation under climate change conditions for a Northern Water Resources System. **Water Resources Management**, Reidel, v. 28, n. 13, p. 4631-4644, 2014.

HARTMANN, H. C.; BALES, R.; SOROOSHIAN, S. **Weather, climate, and hydrologic forecasting for the southwest U.S**. Tucson: The University of Arizona, 1999. 172p. (Working Paper Series, WP2-99).

HASAN, M.M.; WYSEURE, G. Impact of climate change on hydropower generation in Rio Jubones Basin, Ecuador. **Water Science and Engineering**, v. 11 (2), p. 157–166, 2018.

HO, J. T.; THOMPSON, J. R.; BRIERLEY, C. Projections of hydrology in the Tocantins-Araguaia Basin, Brazil: uncertainty assessment using the CMIP5 ensemble. **Hydrological Sciences Journal**, Oxford, v. 61, n. 3, p. 1-17, 2016.

INTERGOVERNMENTAL PANEL ON CLIMATE CHANGE. **Emissions scenarios for the IPCC**: an update. Cambridge: Cambridge University, 2007.

INTERGOVERNMENTAL PANEL ON CLIMATE CHANGE. **Climate Change 2013: The Physical Science Basis**. Working Group I Contribution to the Fifth Assessment Report of the IPCC. Cambridge: Cambridge University, 2013.

INTERGOVERNMENTAL PANEL ON CLIMATE CHANGE. **Climate Change 2014: Impacts, Adaptation, and Vulnerability**. Part A: Global and Sectoral Aspects. Cambridge: Cambridge University, 2014.

INTERNATIONAL ENERGY AGENCY. **Electricity information**: overview 2017. Disponível em: <www.iea.org/statistics/topics/electricity/>. Acesso em: 15 Nov. 2017.

KAWAZOE, S.; GUTOWSKI, W. J. Regional, Very Heavy Daily Precipitation in CMIP5 Simulations. **Journal of Hydrometeorology**, v. 14, p. 1228-1242. 2013.

LEHNER, B.; CZISCH, G.; VASSOLO, S. The impact of global change on the hydropower potential of Europe: a model-based analysis. **Energy Policy**, Surrey, v. 33, n. 7, p. 839-855, 2005.

LIU, W. et al. Impacts of climate change on hydrological processes in the Tibetan Plateau: a case study in the Lhasa River basin. **Stochastic Environmental Research and Risk Assessment**, Berlin, v. 29, p. 1809-1822. 2015.

LOBANOVA, A. et al. Impacts of changing climate on the hydrology and hydropower production of the Tagus River basin. **Hydrological Processes**, Chichester, 2016.

MAJONE, B. et al. Impact of climate change and water use policies on hydropower potential in the south-eastern Alpine region. **Science of the Total Environment**, Amsterdam, v. 543(B), p. 965-980, 2016.

MARENGO, J. A. et al. Future change of climate in South America in the late twenty-first century: intercomparison of scenarios from three regional climate models. **Climate Dynamics**, Berlin, v. 35, n. 6, p. 1073-1097, 2010.

MARENGO, J. A. et al. Development of regional future climate change scenarios in South America using the Eta CPTEC/HadCM3 climate change projections: Climatology and regional analyses for the Amazon, São Francisco and the Parana River Basins. **Climate Dynamics**, Berlin, v. 38, p. 1829–1848, 2012.

MARENGO, J. A. et al. Future change of temperature and precipitation extremes in South America as derived from the PRECIS regional climate modeling system. **International Journal of Climatology**. Chichester, v. 29, p. 2241- 2255, 2009.

MARINHO FILHO, G. M. et al. Modelos hidrológicos: conceitos e aplicabilidades. **Revista de Ciências Ambientais**, v. 6, n. 2, p. 35-47, 2012.

MELLO, C. R. et al. Development and application of a simple hydrologic model simulation for a Brazilian headwater basin. **Catena**, Amsterdam, v. 75, n. 3, p. 235-247, 2008.

MENÉNDEZ, C. et al. Downscaling extreme month-long anomalies in southern South America. **Climate Change**, Berlin, v. 98, p. 379–403, 2010.

MINVILLE, M. et al. Adaptation to climate change in the management of a Canadian water-resources system exploited for hydropower. **Water Resources Management**, Reidel, v. 23, n. 14, p. 2965-2986, 2009.

MOHOR, G. S. et al. Exploratory analyses for the assessment of climate change impacts on the energy production in an Amazon run-of-river hydropower plant. **Journal of Hydrology**: Regional Studies, Amsterdam, v. 4, p. 41-59, 2015.

MOURÃO, C.; CHOU, S. C; MARENGO, J. Downscaling Climate Projections over La Plata River Basin. **Atmosphere and climate sciences**, v. 6, p. 1-12, 2016.

NEELING, J. D. **Climate Change and Climate Modeling**. Cambridge University Press, UK. 2011. 282 p

NEITSCH, S. L. et al**. Soil and water assessment tool**: theoretical documentation version 2005. Temple: Blackland Research Center, 541 p., 2005.

NEUKOM, R. et al. No evidence for globally coherent warm and cold periods over the preindustrial Common Era. **Nature**, London, v. 571, p. 550-572, 2019.

NÓBREGA, M. T. et al. Uncertainty in climate change impacts on water resources in the Rio Grande Basin, Brazil. **Hydrology and Earth System Sciences**, Göttingen, v. 15, p. 585-595, 2011.

NUÑEZ, M. N.; SOLMAN, S. A.; CABRÉ, M. F. Regional Climate change experiments over southern South America. II: climate change scenarios in the late twenty-first century. **Climate Dynamics**, Berlin, 2008.

OLIVEIRA, V. A. et al. Assessment of climate change impacts on streamflow and hydropower potential in the headwater region of the Grande river basin, Southeastern Brazil. **International Journal of Climatology**, Chichester, v. 37, p. 5005-5023, 2017.

OPERADOR NACIONAL DO SISTEMA ELÉTRICO. **O Sistema Interligado Nacional** - SIN. 2017. Disponível em: <http://ons.org.br/pt/paginas/sobre-osin/o-que-e-o-sin>. Acesso em: 15 dez. 2017

OUYANG, F. et al. Impacts of climate change under CMIP5 RCP scenarios on streamflow in the Huangnizhuang catchment. **Stochastic Environmental Research and Risk Assessment**, Berlin, v. 29, p. 1781-1795. 2015.

PATRO, E.R.; MICHELE, C.; AVANZI, F. Future perspectives of run-of-the-river hydropower and the impact of glaciers' shrinkage: The case of Italian Alps. **Applied Energy**, v. 231, p. 699-713, 2018.

PEREIRA, D. dos R. Simulação Hidrológica na bacia hidrográfica do rio Pomba usando o modelo SWAT. 2013. 142p. **Tese** (Doutorando em Engenharia Agrícola). Universidade Federal de Viçosa, Viçosa, 2013.

RENNÓ, C. D. Construção de um sistema de análise e simulação hidrológica: aplicação a bacias hidrográficas. 2003. 146p. **Tese** (Doutorado em Sensoriamento Remoto) - Instituto Nacional de Pesquisas Espaciais, São José dos Campos, 2003.

RENNÓ, C. D.; SOARES, J. V. **Modelos hidrológicos para gestão ambiental**. Programa de Ciência e Tecnologia para Gestão de Ecossistemas - relatório técnico parcial. MCT/INPE, 2000.

ROCHA, R. P. et al. Precipitation diurnal cycle and summer climatology Assessment over South America: an evaluation of Regional Climate Model version 3 simulations. **Journal Geophyshics Research**, v. 114, p. 1-19, 2009

SCHAEFFER, R. et al. Energy sector vulnerability to climate change: a review. **Energy**, Oxford, v. 38, 1, p. 1-12, 2012.

SHAW, E. M. Hydrology in practice. 3rd ed. London: Chapman and Hall, 2004. 569 p.

SILVA, B. C.; TUCCI, C. E. M.; COLLISCHONN, W. Previsão de vazão com modelos hidroclimáticos. **Revista Brasileira de Recursos Hídricos**, Porto Alegre, v. 11, n. 3, p. 15-29, 2006.

SIQUEIRA JÚNIOR, J.L.; TOMASELLA, J.; RODRIGUEZ, D.A. Impacts of future climatic and land cover changes on the hydrological regime of the Madeira River basin. **Climatic Change**, Dordrecht, v. 129 (1-2), p.117–129, 2015

SOARES, W. R.; MARENGO J. A. Assessments of moisture fluxes east of the Andes in South America in a global warming scenario. **International Journal of Climatology**, Chichester, v. 29, p. 1395-1414, 2009.

SOLMAN, S. A.; NUÑEZ, M. N.; CABRÉ, M. F. Regional climate change experiments over southern South America. I: present climate. **Climate Dynamics**, Berlin, v. 30, p. 533–552, 2008.

SOROOSHIAN, S. et al. **Hydrological modelling and the water cycle**. Springer: Heidelberg, 2008. 291 p.

SOUZA, L. R. et al. Experimentação e simulação hidrológica aplicada ao uso de energia hidrocinética na bacia do Rio Maracá – Amapá. **Engenharia Ambiental**, Espírito Santo do Pinhal, v. 8, n. 1, p. 110-125, 2011.

SUN, S. et al. On the attribution of the changing hydrological cycle in Poyang Lake Basin, China. **Journal of Hydrology**, Amsterdam, v. 514, p. 214-225. 2014.

TAN, M. L. et al. Climate change impacts under CMIP5 RCP scenarios on water resources of the Kelantan River Basin, Malaysia. **Atmospheric Research**, Amsterdam, v. 189, p. 1-10, 2017.

TUCCI, C. E. M. **Modelos hidrológicos**. 2. ed. Porto Alegre: UFRGS, 2005. 678 p.

TEUTSCHBEIN, C.; WETTERHALL, F.; SEIBERT, J. Evaluation of different downscaling techniques for hydrological climate-change impact studies at the catchment scale. **Climate Dynamics**, Berlin, v. 37, p.2087-2105, 2011.

VAN VLIET, M.T.H. et al. Power-generation system vulnerability and adaptation to changes in climate and water resources**. Nature Climate Change**, v. 6 (4), p. 375-381, 2016.

VAUTARD R. et al. The simulation of European heat waves from an ensemble of regional climate models within the EURO-CORDEX project. **Climate Dynamics**, Berlin, v. 41, p. 2555–2575, 2013.

VIOLA, M. R. Simulação hidrológica na região Alto Rio Grande a montante do Reservatório de Camargos/CEMIG. 2008. 120 p. **Dissertação** (Mestrado em Engenharia de Água e Solo) - Universidade Federal de Lavras, Lavras, 2008.

VIOLA, M. R. Simulação hidrológica na cabeceira da bacia hidrográfica do Rio Grande de cenários de uso do solo e mudanças climáticas A1B. 2011. 286p. **Tese** (Doutorado em Engenharia de Água e Solo) Universidade Federal de Lavras, Lavras, 2011.

VIOLA, M. R. et al. Applicability of the Lash model for hydrological simulation of the Grande River Basin, Brazil. **Journal of Hydrologic Engineering**, Reston, v. 18, p. 1639–1652, 2013.

VIOLA, M. R. et al. Impacts of Land-use Changes on the Hydrology of the Grande River Basin Headwaters, Southeastern Brazil. **Water Resources Management**, Reidel, v. 28, p. 4537–4550, 2014.

VIOLA, M. R. et al. Assessing climate change impacts on Upper Grande River Basin hydrology, Southeastern Brazil. **International Journal of Climatology**, Chichester, v. 35, p. 1054–1068, 2015.

ZHANG, Y. et al. Impacts of climate change on streamflows under RCP scenarios: A case study in Xin River Basin, China. **Atmospheric Research**, v. 178, p. 521-534, 2016.

ZHAO, D.; LIU, J. A new approach to assessing the water footprint of hydroelectric power based on allocation of water footprints among reservoir ecosystem services. **Physics and Chemistry of the Earth**, Bristol, v. 79/82, p. 40-46, 2015.

SEGUNDA PARTE – ARTIGOS

ARTIGO 1 - SOIL WATER STORAGE ESTIMATE USING A HYDROLOGICAL MODEL PERFORMED WITH HYDROLOGICAL RESPONSE UNITS

ABSTRACT: The use of hydrological models to simulate water budget components is one of the main potential tools for water resources management. Hydrological models can predict the fluvial regime of the basins along with other hydrological variables, such as the soil water storage and evapotranspiration. The Lavras Simulation of Hydrology (LASH) model was developed to be applied at watersheds with scarce input variables and focused on the continuous streamflow simulation. This study aimed to use Hydrological Response Units (HRUs) in the LASH model structure to improve its calibration and validation in a daily time step, and to assess the model's capability for simulation, streamflows and soil water storage, considering or concept in the hydrological units of the basin. LASH model was calibrated and validated to Grande river basin upstream from Furnas Hydropower Plant (GRB-Furnas), in southeastern Brazil. Nash-Sutcliff coefficient (C_{NS}) and its logarithmic version were analyzed in both calibration and validation to appraise LASH's performance in a daily time step. It was obtained C_{NS} of 0.86 and 0.77, respectively, for calibration and validation. Comparing the precision statistics obtained by other hydrological simulation studies conducted in GRB with LASH model, the use of the HRUs produced significant improvements on the simulations, highlighting the peak streamflows estimates. Also, the calibrated parameters showed a good relationship with the hydrological processes within the HRUs, reducing their empiricism. Soil water storage estimates reflect the geomorphological, climate and land-use of the sub-basins, showing the greater influence of the pedological units and land-use, respectively, in the average (long-term soil moisture) and maximum soil water storage.

KEYWORDS: hydrological models, hydrological models calibration, spatial variability, hydrological processes.

1. INTRODUCTION

Many practical aspects of the natural resource management are influenced by the hydrological regime in tropical ecosystems (LIU; WANG; LI, 2014; SHI, 2013). The understanding the practical applications of the hydrological cycle has been recently boosted by the advance of the hydrological models with the support of the GIS, which have been employed for water resources management in watersheds (BESKOW et al., 2016; VIOLA et al., 2013).

Rainfall-runoff models are used to assist in solving several problems in the hydrological engineering, such as to estimate water availability, to forecast streamflows, to assess the hydrological responses of the watershed caused by changes in the land-use, climate and water consumption. Therefore, hydrological modeling has settled as a tool to water resources management and supporting making-decisions, as well as to understand the hydrological processes involved with the water balance in basins (BESKOW et al., 2016). Besides, the soil water storage simulation in the spatial units emerges as a promising output of the hydrological models, whose applicability to irrigation and soil and water conservation projects is relevant.

The "Lavras Simulation of Hydrology" (LASH) was used in this study since it has shown great performance in several Brazilian basins (BESKOW; MELLO; NORTON, 2011; BESKOW et al., 2016; CALDEIRA et al., 2019; VIOLA et al., 2012, 2013). It is a deterministic, semi-conceptual, spatial distributed (by sub-basins or cells) and long-term hydrological model. Its first version was presented by Viola (2008) and Mello et al. (2008) aiming to simulate the hydrology of the basins with scarce hydro-meteorological datasets (CALDEIRA et al., 2019).

Mello et al. (2008) calibrated the LASH model for the first time to two basins in Upper Grande river basin, southeastern Brazil, using two spatial approaches, lumped and distributed by sub-basins. They evaluated an acceptable performance of the model in both approaches, although the

distributed one had shown better estimates of the peak flows. Yet, the model was used to simulate hydrological impacts caused by changes in the land-use in these sub-basins, and the authors concluded that the model was able to adequately simulate the hydrological processes involved with changes in vegetation, since it is based on the vegetative parameters (aerodynamical and stomatal resistance, leaf area index) and considers the mean root depth of the vegetation in the water balance.

Beskow (2009) and Beskow, Mello and Norton (2011) presented the second version of the LASH model. They introduced a Geographical Information System framework to establish a cells scheme approach along with an automatic calibration procedure, the Shuffled Complex Evolution (SCE-UA) (DUAN; SOROOSHIAN; GUPTA, 1992). This new spatial approach resulted in a good performance of the model for daily streamflow simulation in a watershed representative of the Latosols in southeastern Brazil. Beskow, Mello and Norton (2011) assessed the sensitivity of the LASH model parameters in the cited watershed and verified that the parameters related to the baseflow and direct surface runoff the most sensitive. Using the 2nd version of LASH, Beskow et al. (2016) modeled a basin in southern Brazil, with a good performance for daily streamflow simulation.

The 3rd version of the LASH model was presented by Caldeira (2016). The main novelties were advances in computational procedures for processing the temporal and spatial datasets by means specific modules for the sub-basins spatial approach. Using this version, Caldeira et al. (2019) compared two spatial approaches of the LASH model, sub-basins and cells, to Fragata river basin, in southern Brazil. The results showed good performance of both spatial discretization, however, the framework of the cells presented better performance to simulate daily streamflows.

Nonetheless, the concept of Hydrological Response Units (HRUs) has not been yet tested in the LASH model structure. HRUs have been implemented in the hydrological modeling with the advance of GIS tools, e.g. the Soil and Water Assessment Tool model (SWAT). SWAT requires

information in three levels of the spatial scale: watershed; sub-watershed and HRU. HRU is a geomorphological approach that classifies different areas within the basin combining topography, soils, and land-use, independently of its geographical location (NEITSCH et al., 2005).

The sub-watersheds divided into HRUs become possible to simulate the evapotranspiration resultant from different combinations of crops and soil types. The runoff is calculated for each HRU, routed in sub-watersheds level, and then accounted for the watershed. According to Neitsch et al. (2011), the use of HRUs may produce a better physical simulation of the water balance and increase the accuracy of the streamflow estimates in the watershed. Thus, its implementation has potential to improve the LASH model's physical structure.

The use of HRUs in the LASH model will allow simulating the water balance from specific combinations of vegetation, soils, and topography. Other hydrological outputs than streamflow will be accessed, highlighting the soil water storage (SWS). SWS can be useful to several soil and water engineering purposes, such as irrigation design and management, harvest planning, and forecasting the hydrological and agronomic droughts. This study objectives to use HRUs in LASH model to increase the models' performance in simulation the streamflow and the soil water storage behavior throughout the time and spatially by sub-basins.

2. MATERIALS AND METHODS

2.1 The LASH Model

The Lavras Simulation of Hydrology (LASH) is a semi-conceptual hydrological model. It is based on the CN-SCS modified by Mishra et al. (2003), Linear Muskingum-Cunge routing model (CUNGE, 1969) and the porous media flows according to Brooks and Corey equations (RAWLS et al., 1993), among others.

LASH is structured based on three basic modules: i) the direct surface runoff (D_{SUP}), sub-surface runoff (D_{SS}) and baseflow (D_B) quantification; ii) the second module simulates the time lag of the streamflows in the reservoirs; iii) the flows are routed in the drainage network using the Muskingum-Cunge Linear model (CUNGE, 1969).

The water balance in the LASH model is calculated as follows:

$$\frac{\Delta SWS}{\Delta t} = SWS_{t+1} - SWS_t = \left(P - D_{sup} - D_{ss} - D_B - ET\right)\Delta t \quad (1)$$

Where SWS_{t+1} is the soil water storage in the time step "t+1" (L); SWS_t is the soil water storage in the previous time t (L); P is the precipitation less canopy interception (L T^{-1}); D_{SUP} is the direct surface runoff (L T^{-1}); D_{SS} is the subsurface runoff (L T^{-1}); D_B is the baseflow (L T^{-1}); ET is the evapotranspiration (L T^{-1}); and ΔT is time step of the simulation (T).

Canopy interception is calculated in the LASH model considering the maximum canopy storage (Imax) given by (ALMEIDA et al., 2007; COLLISCHONN, 2001; COLLISCHONN et al., 2007; MELLO et al., 2008; ZHOU et al., 2006):

$$I_{max} = \alpha LAI \quad (2)$$

Where α is the interception coefficient (dimensionless), assumed to be 0.2 mm (COLLISCHON et al., 2007; DICKINSON, 1984; WIGMOSTA; VAIL; LETTENMAIER, 1994) and LAI is the leaf area index (m^2 m^{-2}).

For the calculation of the water evaporation from canopy and transpiration from vegetation, LASH model uses the Penman-Monteith equation that considers as inputs the vegetation covering parameters (albedo, high of the trees and aerodynamic and stomatic resistances) and meteorological datasets (ALLEN et al., 1998).

According to Viola et al. (2009), it is required a coefficient (ks) for correction of the evapotranspiration so that soil moisture reduction is taken into consideration. Conceptually, evapotranspiration is exponentially reduced

from a critical threshold of the soil water storage (SWS_c), being the lowest value the moisture correspondent to the permanent wilting point (SWS_{pwp}). Shuttleworth (1993) suggests for SWS_{pwp} and SWS_c, respectively, 10% and 50% of the maximum SWS.

Direct surface runoff (D_{SUP}) is estimated based on the CN-SCS method modified by Mishra et al. (2003). This method was changed to physically improve the Initial Abstraction of precipitation (Ia) and the maximum soil water storage (S) relationship, using the precipitation in the last 5 days (P5) to describe the antecedent soil moisture influence. D_{SUP} is estimated by:

$$D_{SUP} = \frac{(P - I_a)(P - I_a + M)}{P - I_a + M + S} \quad (3)$$

Where P is the precipitation (L T^{-1}); I_a is the initial abstraction of precipitation (L T^{-1}); M is the antecedent soil moisture (L T^{-1}); and S is the maximum soil water storage (L T^{-1}).

Sub-surface runoff (D_{SS}) is calculated using the Brooks and Corey equation (RAWLS et al., 1993) for modeling the fluxes in porous media:

$$D_{SS} = K_{SS}\left(\frac{SWS_{t-} SWS_{cc}}{SWS_{m-} SWS_{cc}}\right)^{\left(3+\frac{2}{m}\right)} \quad \text{if} \quad SWS_t \geq SWS_{cc} \quad (4)$$

$$D_{SS} = 0 \quad \text{if} \quad SWS_t < SWS_{cc} \quad (5)$$

K_{SS} is the hydraulic conductivity of the sub-superficial reservoir, being a calibration parameter (L T^{-1}); m is the soil porosity index (dimensionless) and SWS_{cc} is the minimum water storage from which the sub-surface flow begins (L).

The base flow (D_b) is also estimated based on the Brooks and Corey equation (RAWLS et al., 1993):

$$D_B = K_B \left(\frac{SWS_{t-} SWS_c}{SWS_{m-} SWS_c} \right) \quad \text{if} \quad SWS_t \geq SWS_c \quad (6)$$

$$D_B = 0 \quad \text{if} \quad SWS_t < SWS_c \quad (7)$$

K_B is the hydraulic conductivity of the groundwater reservoir, being a calibration parameter (L T^{-1}); SWS_c is the minimum soil water storage in the groundwater reservoir from which the baseflow begins.

LASH model converts the surface runoff components into discharge considering linear reservoirs in each sub-basin, taking the time lag of the fluxes, which means the time to water leaves the reservoirs and reaches the drainage network. The following equations are used:

$$Q_{SUP} = \frac{D_{\sup} A_{sub-bacia}}{C_{\sup} T_c} = \frac{V_{SUP}}{C_{SUP} T_c} \quad (8)$$

$$Q_{SS} = \frac{D_{ss} A_{sub-bacia}}{C_{SS} T_c} = \frac{V_{SS}}{C_{SS} T_c} \quad (9)$$

$$Q_B = \frac{D_B A_{sub-bacia}}{T_B} = \frac{V_B}{T_B} \quad (10)$$

Where Q_{SUP}, $Q_{SS,}$ and Q_B are the direct surface runoff, the sub-superficial runoff and the baseflow, in L^3T^{-1}; $A_{sub\text{-}basin}$ is the drainage area of the sub-basins derived from the DEM (L^2); V_{SUP}, V_{SS} and V_B are the volumes, respectively, from the surface, sub-surface and groundwater reservoirs (L^3); T_C is time of concentration (T); T_B is the recession time of the hydrograph (T); C_{SUP} and C_{SS} are the routing calibration parameters (dimensionless).

The Tb parameter was calculated based on the recession phase of the hydrographs of the sub-basins that have a stage-discharge gauge station. For the sub-basins without these stations, Tb was regionalized using regression between Tb and the drainage area of the sub-basins.

For streamflow routing in the drainage network, the Muskingum-Cunge linear method is used (CUNGE, 1969). This method considers the

physical characteristics of the channels, such as width, steepness, bed roughness, celerity, and discharge. The method is mathematically described as follows (TUCCI, 2005):

$$Q_s^{t+1} = C_1 \cdot Q_i^{t+1} + C_2 \cdot Q_i^t + C_3 \cdot Q_s^t \quad (11)$$

Where Q_S is the routed discharge (L^3T^{-1}) at the end of the channel between the times "t+1" and "t"; Q_i is the input discharge in the beginning of the channel; C_1, C_2 and C_3 are the routing constants (dimensionless).

2.2 The studied basin

The studied basin is the Upper-Middle Grande river, southeastern Brazil, which was delineated upstream from Furnas Hydropower Plant (GRB-Furnas) (geographical coordinates 20° 40' S and 40° 20' W), with a drainage area of 51,852 km^2 (FIGURE 1). The elevation varies from 2771 m to 657 m.

The climate of the basin, according to Köppen climate classification, is Cwa in middle and Cwb in the upper region of the basin (Mantiqueira Range and surroundings). Both climates are characterized by two well defined seasons, one warm and wet (spring/summer) and other dry and cool (autumn/winter). Mean annual precipitation varies from 1,600 mm to 2,300 mm (Bueno et al. 2017), mean annual temperature is approximately 18^{o}C and average minimum and maximum temperatures are, respectively, 11^{o}C (July) and 21^{o}C (January) (MELLO et al., 2012).

Figure 1 – Geographical location of the Grande river basin in Brazilian territory, the Upper-Middle Grande river basin upstream Furnas Hydropower Plant (GRB-Furnas), and the fluviometric gauges, rain gauges and meteorological stations.

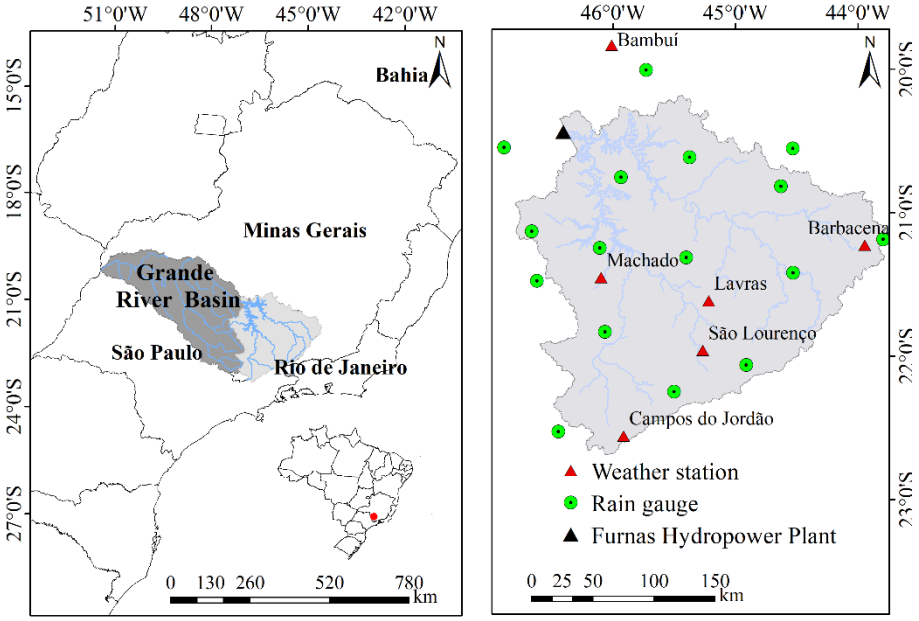

Source: From author (2019).

2.3 Maps and hydrometeorological database

A daily hydrometeorological database was structured for calibration, validation and application of the LASH model, using the Thiessen Polygon Method for calculation of the spatial average value. Figure 1 shows the geographical location of the fluviometric and rain gauges and meteorological stations used in this study. Meteorological stations belong to the "Instituto Nacional de Meteorologia" (INMET/BDMEP) and are located at the municipalities of Lavras, São Lourenço, Barbacena, Machado, Bambuí, and Campos do Jordão. Rainfall datasets were obtained from HidroWeb "Sistema de Informação Hidrológica" from the "Agência Nacional das Águas" (HidroWeb/ANA) and the streamflows from "Operador Nacional do Sistema Elétrico" (ONS). For calibration and validation of the LASH model, it was

used naturalized streamflows from Furnas Hydropower Plant, which are simulated using 96 stochastic models excluding the reservoir and water withdrawals for consumptive uses (GUILHON; ROCHA; MOREIRA, 2007; ONS, 2008; OLIVEIRA et al., 2019).

The need information for characterization of the spatial units in the LASH model is the Digital Elevation Model (DEM), which was adopted from ASTER (Advanced Spaceborne Thermal Emission and Reflection Radiometer) with 30 meters of spatial resolution (FIGURE 2a). The ArcGIS software was used to obtain a hydrologically consistent DEM and to derive the drainage network, slope map (FIGURE 2b) and delimitation of the sub-basins (FIGURE 2c,d).

For calibration and validation of the LASH model, the land use and soil maps are required. The land use map is presented in Figure 2c and was derived based on the LANDSAT 8 images of 2018. The pasture is the dominant land-use (40.76%), followed by Atlantic Forest (25.07%), agriculture (18.17%) and Brazilian Savanna (Cerrado) (9.88%). Other land-uses account for 6.12%, corresponding to water bodies, eucalyptus, urban areas, and bare soils.

Soil map (FIGURE 2d) was obtained from “Fundação Estadual do Meio Ambiente de Minas Gerais” in a scale 1: 650,000 (FEAM, 2010). The Latosol are predominant (42.96%), followed by Argisols (25.76%), Cambisol (23.08%) and Litholic Neosol (3.27%). Other classes were observed, however, accounting only 4.93% of the basin’s area.

Figure 2 – Digital elevation model (a) and maps of slope (b); land-use (c); soils; (d) and the spatial discretization by sub-basins (c, d) of the GRB-Furnas; and sub-basins chosen to study the temporal soil moisture (1, 2, 3).

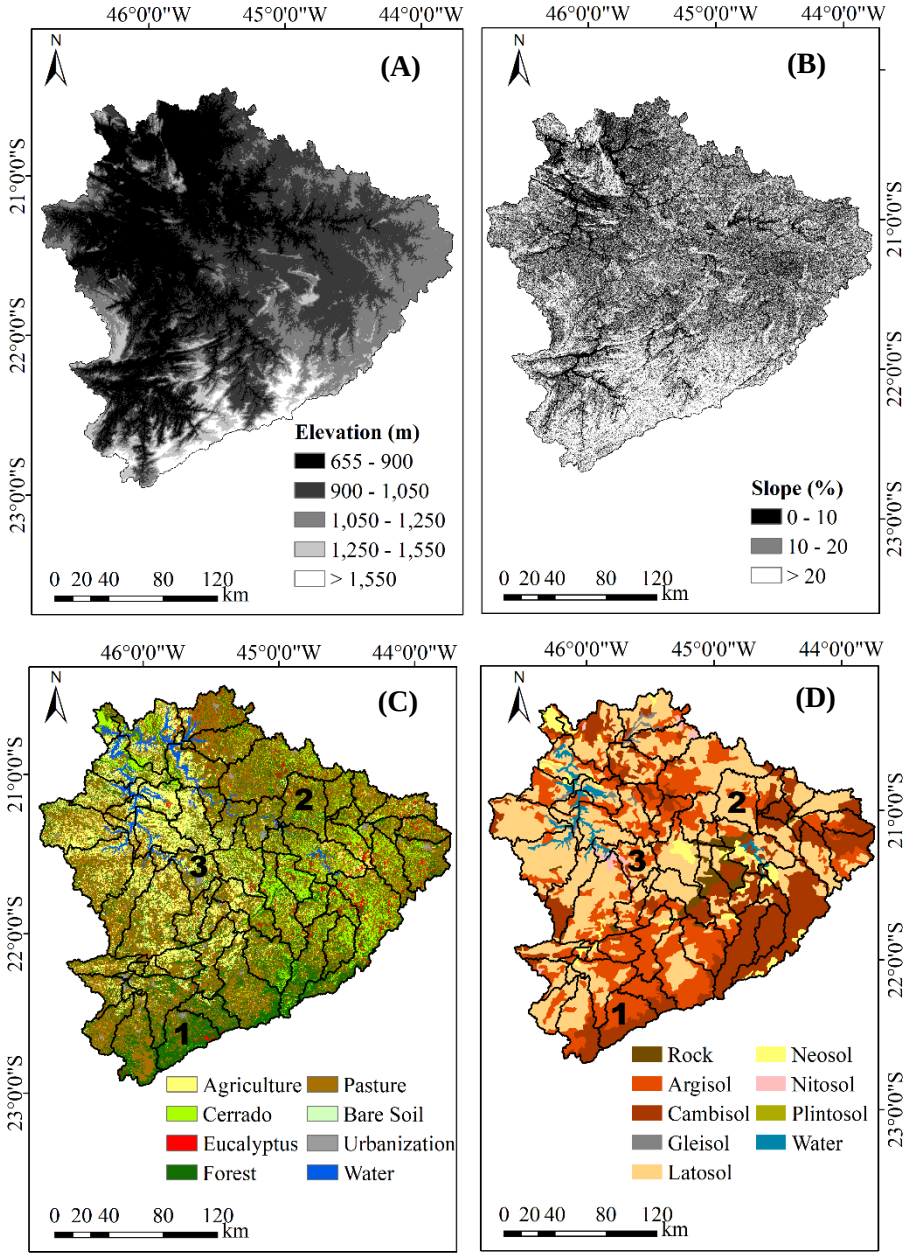

Source: From author (2019).

2.4 Calibration and validation of the LASH model using HRUs

The calibration and validation of the LASH model were carried out aiming to maximize the Nash-Sutcliffe coefficient (NASH; SUTCLIFFE, 1970), considering the daily streamflows in a period of 18 years (1990- 2007). At the beginning of the simulation, there are uncertainties associated with the initial hydrological conditions, especially the soil moisture initial behavior. To overcome this, the hydrological modeling procedures recommend using an initial period to warm up the model, in both calibration and validation (COLLISCHONN et al., 2007; MELLO et al., 2008; STACKELBERG et al., 2007). It was used the years of 1990 and 2000, respectively, to warm-up the calibration and validation.

In this study, LASH was calibrated using the concept of Hydrological Response Units (HRUs). HRUs are defined as unique combinations of the land-use, soils, and slope, and were generated individually for each sub-basin. The predominant classes criterion (NEITSCH et al., 2005) was used for the HRU generation. According to this criterion, each sub-basin will have only one HRU. Soil, vegetation and slope classes that predominate in the sub-basin will define the respective HRU. A total of 69 sub-basins were defined in GRB-Furnas area, identifying 21 different combinations of HRUs, following the classes in Table 1. Sub-basins with the same HRU will have the same set of the parameters.

Table 1 – Soil, vegetation and slope classes used to structure the HRUs in GRB-Furnas.

Soil	**Slope (%)**	**Vegetation**
Latosol – Bw	0 – 10	Atlantic Forest
Argisol – Bt	10 - 20	Cerrado
Cambisol – Bi	>20	Pasture
Litholic Neosol – Ne	-	Agriculture
Rock - R	-	-

Source: From author (2019).

The calibration parameters of the LASH model are (MELLO et al., 2008): Initial Abstraction of the precipitation (λ); hydraulic conductivity of the sub-surface reservoir (K_{SS} - mm day^{-1}); hydraulic conductivity of the groundwater reservoir (K_B – mm day^{-1}); and routing coefficients of the surface and sub-surface reservoirs (C_{SUP} and C_{SS}, respectively). In Table 2, it is presented the boundaries considered for calibration of the LASH parameters.

Table 2 – LASH model calibration parameters and respective boundaries.

Parameter	Bound	Reference
λ	0 a 0.5	Mishra et al. (2003)
K_{SS}	0 a 182.4	Rawls et al. (1993)
K_B	0 a 6	Beskow (2009)
C_{SUP}	$C_{SUP} < C_{SS}$	Mello et al. (2008)
C_{SS}	$C_{SUP} < C_{SS}$	Mello et al. (2008)

Source: adapted from the authors cited in the reference column.

The LASH calibration was carried out manually following some assumptions:: i) λ parameter is sensitive to land-use, soil classes and slope of the landscape as they potentially impact the initial abstraction of precipitation (ALVES et al., 2019); ii) K_{SS} is predominately influenced by land-use and slope as sub-surface runoff is more impacted by such features of the landscape (MELLO et al., 2019); iii) K_B is a parameter more affected by soil classes and land-use as baseflow is linked with the groundwater recharge, which is influenced by the soil hydrology and its relationship with the land-use (PINTO et al., 2015); iv) C_{SUP} is influenced by the slope and is used to fit the concentration time of the sub-basin; v) C_{SS} should be greater than C_{SUP} because direct surface runoff is faster than sub-surface runoff. Thus, the parameters were characterized according to the following classes:

- λ values were grouped into the categories Atlantic Forest and Cerrado (preserved areas) and slope < 10%; preserved areas and slope > 10%; managed areas in Latosols (Bw) and Argisols (Bt) and slope < 10%;

managed areas in Cambisols (Bi) and Litholic Neosols (Ne) and slope < 10%; managed areas in Bw and Bt and slope > 10%; and managed areas in Bi and Ne and slope > 10%.

- K_{SS} values were grouped into the categories preserved areas; and slope > 20%; areas with slope between 10 and 20%; and areas with slope between 0% and 10% or associated to rocks;
- K_B values were grouped in preserved areas; managed areas in Bw and Bt; managed areas in Bi; and areas with Ne;
- C_{SUP} values were characterized in accordance with the effects of the slope and grouped into the slopes 0% - 10%; 10% - 20%; and > 20%.

2.5 Assessment of the LASH model performance

The performance of the LASH model was appraised considering the following precision statistics:

- Nash-Sutcliffe (C_{NS}) and its logarithmic version (Log (C_{NS})) (NASH; SUTCLIFFE, 1970); C_{NS} is sensitive to the peak streamflows estimates, whereas log (C_{NS}) is sensitive to the baseflow. Moriasi et al. (2015) proposed for C_{NS} the following classification: $C_{NS} > 0.80$: a "very good" model; $0.70 < C_{NS} \leq 0.80$, a "good" model; $0.50 < C_{NS} \leq 0.70$: "satisfactory" model; and $C_{NS} \leq 0.50$: "unsatisfactory" model.

$$C_{NS} = 1 - \left[\frac{\sum_{i=1}^{n}\left(Q_{OBS_i} - Q_{SIM_i}\right)^2}{\sum_{i=1}^{n}\left(Q_{OBS_i} - \overline{Q_{OBS_i}}\right)^2}\right] \quad (12)$$

$$\log(C_{NS}) = 1 - \left[\frac{\sum_{i=1}^{n}\left(log(Q_{OBS_i}) - log(Q_{SIM_i})\right)^2}{\sum_{i=1}^{n}\left(log(Q_{OBS_i}) - \overline{log(Q_{OBS_i})}\right)^2}\right] \quad (13)$$

- Ratio between observed and calculated volumes (ΔV) (COLLISCHONN, 2001): this statistic indicates the accuracy of the model for estimating the water balance and the evapotranspiration. According to Van Liew, Arnold and Garbrecht (2003), ΔQ values < 10% represent a very good fit, between 10 and 15%, a good fit, between 15 and 25%, satisfactory, and over 25% represent inappropriateness for estimation.

$$\Delta V = \frac{\sum_{i=1}^{n}(Q_{SIM_i}) - \sum_{i=1}^{n}(Q_{OBS_i})}{\sum_{i=1}^{n}(Q_{OBS_i})} . 100 \quad (14)$$

Where Q_{SIM} is simulated streamflow (L^3T^{-1}), Q_{OBS} is observed streamflow, Q_{OBS} is average observed streamflow, and n is number of events.

2.6 Assessment of the soil water storage in the sub-basins

After the calibration and validation of the LASH model, the soil water storage was assessed in two ways: i) three sub-basins were chosen (Figures 2 c, d) considering different dominant HRUs to demonstrate the ability of the model to simulate the soil water storage over the time, being sub-basin 1: Atlantic Forest + Cambisol; sub-basin 2: Pasture + Latosol; sub-basin 3: Agriculture + Latosol. We extracted the temporal behavior of the soil water storage under these geomorphological conditions; ii) average (long-term storage) and maximum soil water storage for all the sub-basins were estimated using the model's output, and two maps were generated, which can be very useful for the land use management and for subsidizing soil and water engineering projects.

3. RESULTS AND DISCUSSION

3.1 Assessment of the LASH model performance using HRUs

The LASH model parameters are presented in Table 3, following the respective classes established for each parameter.

Table 3 – LASH model calibrated parameters using HRUs for GRB-Furnas.

Conditions	**Lambda - λ**
Preserved areas in slope < 10% and all soil classes	0.5
Preserved areas in slope > 10% and all soil classes	0.45
Managed areas in Bw and Bt and slope < 10%	0.4
Managed areas in Ne and Bi and slope < 10%	0.35
Managed areas in Bw and Bt and slope >10%	0.03
Managed areas in Ne and Bi and slope > 10%	0.0185
Conditions	**K_B – mm day^{-1}**
Preserved areas and all soil classes	5
Managed areas in Bw and Bt	4
Managed areas in Bi	2.5
Shallow soils (Ne and rock predominance)	2
Conditions	**K_{SS} – mm day^{-1}**
Preserved areas and all the slope	25
Slope: > 20% and areas maneged	22
Slope: 10% - 20% and areas maneged	20.74
Slope: 0 - 10% and exposed rock	18
Conditions	**C_{SUP} – coefficient**
Slope: 0 - 10%	9
Slope: 10% - 20%	6.01
Slope: > 20%	5
Conditions	**C_{SS} – coefficient**
Slope: 0 - 10%	80
Slope: 10% - 20%	79
Slope: > 20%	75

Source: Source: From author (2019).

The λ parameter models the initial abstraction of the precipitation (Ia), which is defined as the total precipitation between the beginning of the rain and the beginning of the direct surface runoff (MISHRA; SINGH, 2006). Ia affects the direct surface runoff generation, which justifies the calibration of this parameter taking as reference the soil classes, land-use and the slope of the landscape. SCS (1971) recommends a value of 0.20, meaning that Ia corresponds to 20% of the maximum soil water storage capacity. This value

is used in some hydrological models, Such as SWAT. However, its behavior depends on the geomorphological characteristics of the basin, and a calibration procedure can be necessary to better estimate peak atreamflows (ALVES et al., 2019; MISHRA et al., 2003). One can observe in Table 3 that preserved areas combined with slope < 10 greatest value (0.5) for, λ. Such areas tend to produce greater Ia and thus, a lower amount of direct surface runoff and lower peak flows. On the other hand, most of the managed areas with Ne and Bi are associated with greater slopes, and therefore, greater direct surface runoff and higher peak streamflows. For these HRUs, λ was calibrated with the smallest value (0.0185).

K_B and K_{SS} parameters represent the hydraulic conductivity of the sub-surface and groundwater reservoirs, respectively, and are associated with the soil hydrology and the slope of the landscape. Preserved areas present high infiltration capacity, which implies in a reduced direct surface runoff, even in Cambisol (PINTO et al., 2015). However, if these soils were occupied by trampled pastures, they have a greater potential to direct surface runoff generation due to their reduced infiltration capacity. Foram considerados diferentes valores de Tb para cada sub-bacia. Este parâmetro foi calculado para o período de recessão dos hidrogramas de recessão de cada estação pluviométrica, utilizada na área de estudo, e posteriormente foi ajustado uma equação relacionando valor de Tb com área de drenagem.

C_{SUP} and C_{SS} parameters are related to the time of concentration of the sub-basins and then, influence the direct surface runoff dynamics. They are relevant for routing the volume from the reservoirs considered in the LASH model structure. Sub-basins with greater slope tend to generate a faster direct surface runoff than sub-basins characterized by flat topography, showing lower values of C_{SUP} and C_{SS} parameters.

3.2 Calibration and validation of the LASH model using HRUs

The precision statistics from both daily calibration and validation of the LASH model are presented in Table 4. This evaluation is fundamental for the model's performance and application to obtain reliable results of the water balance simulation. In this study, we verified the model's capability for simulation of the streamflows as well as soil water storage due to the physical behavior of the parameters of the model, as above presented.

Table 4 – Precision statistics obtained for the calibration and validation of the LASH model using HRUs for GRB-Furnas.

Application		**Precision statistics**		
		C_{NS}	**Log (C_{NS})**	**ΔV(%)**
Calibration	Daily	0.86	0.83	2.16
Validation	Daily	0.77	0.76	11.44

Source: From author (2019).

We could observe C_{NS} values greater than 0.7, which, in general, qualify the model for streamflows simulation (ZAPPA, 2002). Taking the classification of the hydrological models proposed by Moriasi et al. (2015), LASH model could be evaluated as "very good" and "good", for the calibration and validation, respectively. The C_{NS} values obtained in this study showed that LASH calibrated using HRUs can simulate the peak streamflows with high precision, greastest to Viola et al. (2013) who studied sub-basins of GRB-Furnas, using this model.

Other studies using LASH model have been carried out in different Brazilian regions. Viola et al. (2012) applied it to a basin in the north of Tocantins state, northern Brazil, and obtained C_{NS} of 0.74 and 0.75 respectively, for daily streamflows calibration and validation. Viola et al. (2013) assessed the performance of the LASH in four upstream basins of the GRB-Furnas (Aiuruoca, Grande, Verde, and Sapucaí). They found $C_{NS} > 0.70$ in the calibration and validation of daily streamflows. Comparing the study carried by Viola et al. (2013) to this study (GRB-Furnas), we could observe an increase in the performance of LASH ($C_{NS} > 0.77$ for daily streamflows). Beskow et al. (2016) calibrated and validated the 2nd version of LASH

(distributed by cells) to Fragata river basin, far southern Brazil. They obtained C_{NS} values, of 0.81 and 0.72, respectively, for calibration and validation daily streamflows. In a recent comparative study carried out by Caldeira et al. (2019), the 1st (distributed by sub-basins) and the 2nd (distributed by cells) LASH model versions were applied to the Fragata river basin. These authors obtained C_{NS} of 0.74 and 0.54, respectively, for daily streamflows calibration and validation with the sub-basins spatial approach. In both spatial approaches (sub-basins – CALDEIRA et al., 2019; and cells – BESKOW et al., 2016), the model could be evaluated as "good" performance, however, the 2nd version (cells) showed greater accuracy.

The observed and simulated daily hydrographs in Figure 3 (a. calibration; b. validation) strength the results from precision statistics regarding the LASH model performance. We can see a very good agreement between the daily peak streamflows and baseflows over the time in both calibration and validation, demonstrating the high performance of the model in simulating extreme streamflows.

Another relevant characteristic of hydrological models is that the ability in simulating the baseflows. This is measured with the log (C_{NS}) as it is very sensitive to the recession limb of the hydrographs (VIOLA et al., 2009). In this study, LASH model presented high values of log (C_{NS}) (Table 4), which allow evaluating the model as "very good" and "good" (MORIASI et al., 2015). Such statistic and C_{NS} demonstrate that LASH can adequately simulate the extreme streamflows (baseflow and peak streamflows), which validate it for application to water resources management in GRB-Furnas.

Figure 3 – Observed and simulated daily hydrographs using LASH model to GRB-Furnas using the HRUs approach (a. calibration; b. validation).

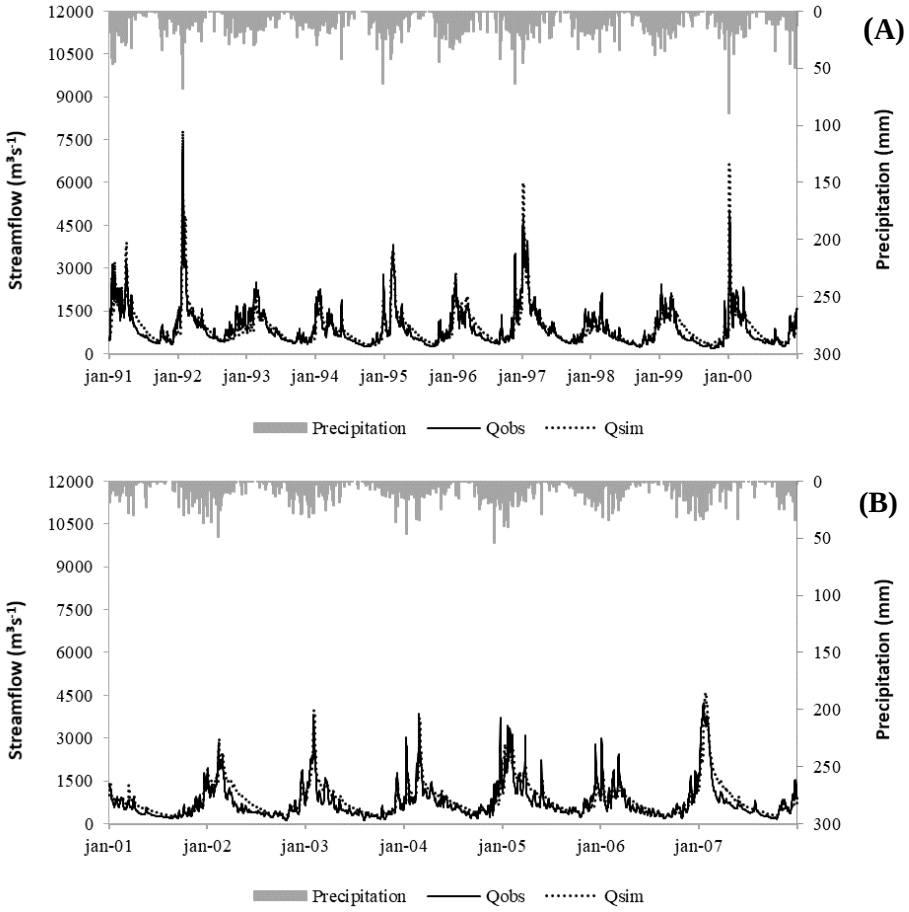

Source: From author (2019).

The ΔV statistic indicates the capability of the hydrological models in estimating the evapotranspiration and in simulating the water balance at the spatial units considered in the model (COLLISCHONN; TUCCI, 2001). LASH model calibrated considering the HRUs presented slight overestimations (up to 11,44%) (TABLE 4), which means a “very good” and “good” performance in water balance simulation, for calibration and validation, respectively (VAN LIEW; ARNOLD; GARBRECHT, 2003). Comparatively, Collischonn and Tucci (2001) calibrated and validated MGB-

IPH model to Taquari-Antas, southern Brazil. They obtained -6.07% and 5.71% and classified these results as good, with reduced errors associated with the water balance simulation. Viola et al. (2013) obtained ΔV varying from -10% to 13% for headwater basins of GRB-Furnas using the LASH model distributed by sub-basins. Based on ΔV values found in this study, the good performance of the LASH model to simulate water balance using HRUs is highlighted, demonstrating that the hydrological processes involved were well simulated.

Comparing the study of Viola et al. (2013) and this one, we could observe the use of HRUs considerable improved the LASH model performance. Both studies were developed in basins of GRB-Furnas, and the superiority of the precision statistics obtained here is quite significant (TABLE 4).

3.3 Soil water storage simulated by the LASH model based on HRUs

Maximum and average (long-term moisture) soil water storage, soil water storage the rain season (Oct to May) and soil water storage the dry season (Jun to Sep) in sub-basins of the GRB-Furnas in the period between 1991 and 2007 are presented in Figure 4. Overlapping these maps and the soil map (FIGURE 2b), one can infer that the average soil water storage (FIGURE 4a) is especially influenced by the pedological characteristics of the soils. Sub-basins with a predominance of Latosols present higher values, whereas in those with a predominance of Cambisols, lower values (ALVARENGA et al., 2012).

Figure 4 – Average soil water storage (a), maximum soil water storage (b) average soil water storage the rain season (c) and average soil water storage the dry season (d) in sub-basins of the GRB-Furnas simulated by the LASH model using HRUs, considering the period of the calibration and validation.

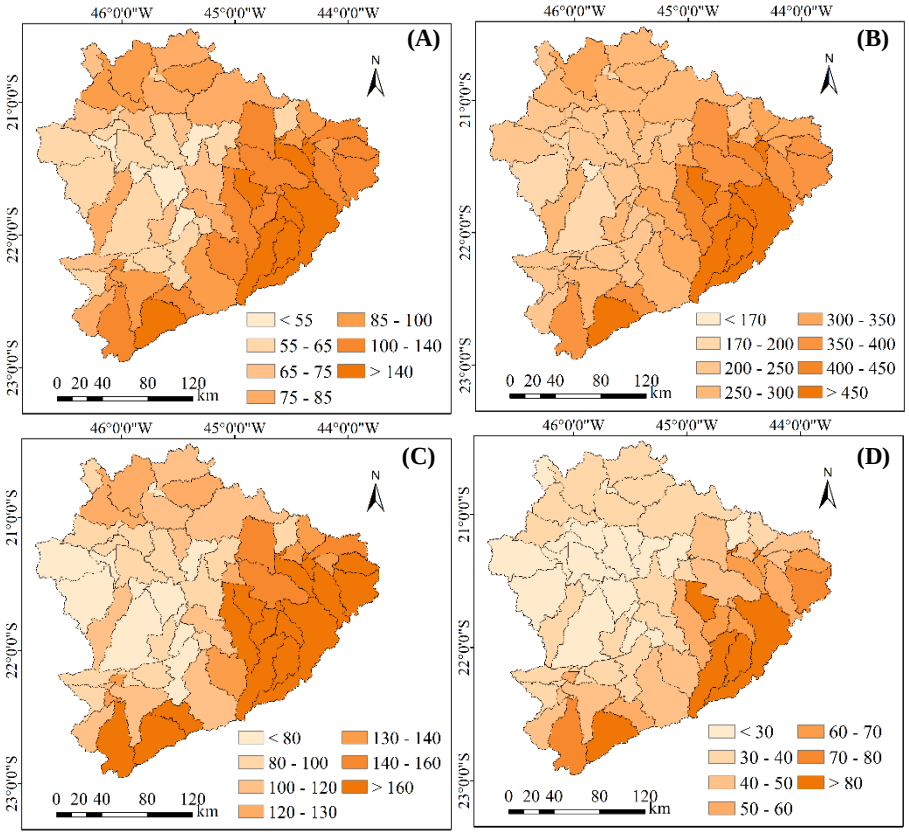

Source: From author (2019).

However, we can also observe that land-use can also affect both average and maximum soil water storage. Relationship between land-use and soil hydrology may influence the movement and redistribution of the water in the soil profile due to organic matter accumulation and development of preferential streamflows (MELLO et al., 2019; PINTO et al., 2015; ZHANG et al., 2015). Analyzing the maps in Figure 4 and Figure 2c (land-use map), the headwater region (south/southeast) of GRB-Furnas showed the greatest values of soil water storage (both average and maximum values), which is a reflex of the Atlantic Forest. However, in southwest and west regions of the

basin, trampled pastures are predominant, independently of the soils, which lead to lower soil water storage. In such sub-basins, the use of the soils can be substantially improved in terms of management, aiming to a balance between production and environment.

Maximum soil water storage is intrinsically related to the soil water infiltration and groundwater recharge. The map in Figure 4b displays that the headwater region of the GRB-Furnas, especially in sub-basins in the southeast region, is more prone to infiltration (MELLO et al., 2019; PINTO et al., 2015), which results in greater soil water storage. This demonstrates that the land use in headwater sub-basins is relevant as the Atlantic Forest dominates most of these sub-basins (FIGURE 2c). Oppositely, we can highlight that in sub-basins dominate by trampled pasture, the lowest maximum soil water storage values were observed. These results demonstrate how these sub-basins have been misused and new strategies for their better management towards to reduce the impacts of the trampled pasture are required.

For characterization of the soil water storage throughout the time, three sub-basins were selected (FIGURE 2c). Such sub-basins were chosen based on the contrasting land uses, soils and slope aiming to appraise how the LASH model simulates the water balance using HRUs and how the soil water storage behaves under different geomorphological situations. These sub-basins were (FIGURE 2c) 1: Cambisols, slope > 30% and Atlantic Forest (FIGURE 5a); 2: Latosols, slope between 0 and 10%, and trampled pasture (FIGURE 5b); and 3: Latosols, slope between 0 and 10% and agriculture (FIGURE 5c).

Figure 5 – Soil water storage throughout the time in three sub-basins under different land-use, soil and relief conditions simulated with LASH model using HRUs.

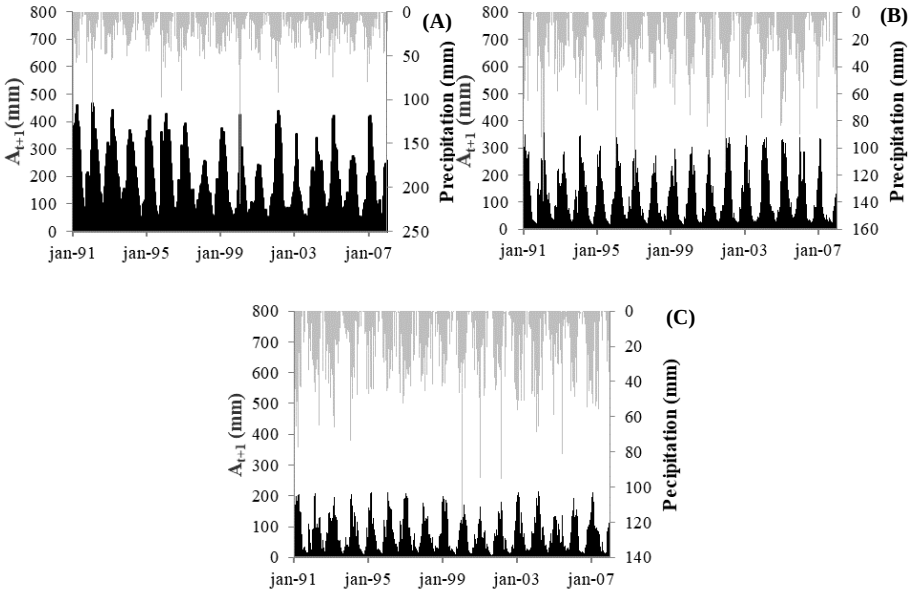

Source: From author (2019).

Table 5 presents the calibrated parameters of the LASH model using the HRUs for the selected sub-basins.

Table 5 – LASH model calibrated parameter for the sub-basins 1, 2 and 3 in the GRB-Furnas.

Calibrated parameters	**Unit**	**Sub-basins**		
		1	**2**	**3**
Λ	-	0.45	0.4	0.4
K_B	mm dia^{-1}	5	4	4
K_{SS}	mm dia^{-1}	25	18	18
C_{SUP}	-	5	9	9
C_{SS}	-	75	80	80

Source: From author (2019).

Sub-basin 1 has greater hydraulic conductivity of sub-surface and groundwater reservoirs, expressed by K_{SS} and K_B. Also, this sub-basin has a

greater initial abstraction of precipitation due to influence of Atlantic Forest, which means lesser direct surface runoff amount than in the other sub-basins.

Sub-basin 1 presents greater soil water storage followed by sub-basins 2 and 3. Maximum soil water storage in the sub-basins was 456 mm, 353 mm and 215 mm, respectively. Despite the predominant soil in sub-basin 1 is Cambisols and the slope is greater 30%, Atlantic Forest influences soil water storage. Pinto et al. (2015), using micromorphological analyzes in Atlantic Forest, observed greater porosity and connectivity between the porous (increasing the soil infiltration capacity), and high organic matter content, which helps to store water in the soil. Mello et al. (2019) studied the water balance in a micro-catchment entirely occupied by Atlantic Forest in the sub-basin 1, using monitored datasets during two hydrological years (2009/2011). Using soil moisture monitored in a layer of 1.0 m, they observed a maximum soil water storage of 550 mm in February of 2011, after a rainfall of 900 mm in January. Average soil water storage observed was 200 mm, whereas LASH simulated 162 mm for sub-basin 1, in the period between 1991 and 2007. Overall, the water balance elements observed in loco by Mello et al. (2019) show similarities with the outputs from LASH, which strength the model capability for soil water storage simulation using the HRUs.

Sub-basins 2 and 3 have a predominance of Latosols, which are deep and clayed soils with greater aggregate stability and undulated and flat topography. Such soils present high infiltration capacity as well as high soil water storage potential. However, they have been used majority for trampled pasture, which can lead to compaction and degradation of the soils, and thus, greater direct surface runoff and less ability to store water (ALVARENGA et al., 2012).

Based on the results presented in Figures 4 and 5, the LASH model's parameters (TABLE 5) are befitting to the hydrological processes involved with the water balance, demonstrating that the use of the HRUs produced reliable results for the GRB-Furnas. The use of HRUs allows increasing the use and applicability of the model for solving several practical problems,

beyond streamflows simulation, conciliating groundwater recharge, livestock production and agriculture. We can highlight data such as water availability for agriculture not only in terms of reference streamflow for water rights but also soil temporal behavior associated with water storage in a daily scale, supporting irrigation designs and management of crops, characterization of droughts using the temporal behavior of the soil water storage, and other environmental problems.

4. CONCLUSIONS

- The precision statistics showed that LASH model calibrated using the HRUs had a great performance in a daily time step highlighting in the estimation of peak flows and baseflows.
- LASH model demonstrated to be a powerful tool to simulate the SWS especially due to the use of HRUs, which improved the model's structure and parametrization and generated reliable results regarding this hydrological variable.
- We could develop maps of the SWS and its temporal behavior in the sub-basins; these outputs is significant for supporting soil and water engineering projects, such as irrigation designs, and crop management, besides advance in the understanding of hydrological droughts.

REFERENCES

ALLEN, R.G. et al. Grop evapotranspiration: guidelines for computing crop water requirements. **Irrigation and Drainage**. Paper No. 56, FAO, Italy, 1998. 328p.

ALMEIDA, A. C. et al. Growth and water balance of Eucalypitus grandis hybrid plantations in Brazil during a rotation for pulp production. **Forest Ecology and Management**, Amsterdam, v. 251, n. 1/2, p. 10-21, 2007.

ALVARENGA, C.C. et al. Índice de qualidade do solo associado à recarga de água subterrânea (IQS_{RA}) na Bacia Hidrográfica do Alto Rio Grande,

MG. **Revista Brasileira de Ciencias do Solo**, Viçosa, v. 36, n.5, p.1608-1619, 2012.

ALVES, G.J. et al. Assessment of the Soil Conservation Service-Curve Number method performance in a tropical oxisol watershed. **Journal of Soil and Water Conservation,** Ankeny, v. 74, p.500-512, 2019.

ARNOLD, J. G. et al. Large area hydrologic modeling and assessment part I: model development. **Journal of the American Water Resources Association**, Herndon, v.34, p.73-89, 1998.

BESKOW, S. LASH model: a hydrological simulation toll in gis framework. 2009. 118 f. **Thesis** (Doctor in Engineering Agricultural) - Universidade Federal de Lavras, Lavras, 2009.

BESKOW, S.; MELLO, C. R.; NORTON, L. D. Development, sensitivity and uncertainty analysis of LASH model. **Scientia Agricola**, Piracicaba, v. 68, n. 3, p. 265-393, 2011.

BESKOW, S. et al. Performance of a distributed semi-conceptual hydrological model under tropical watershed conditions. **Catena**, Amsterdam, v. 86, n. 3, p. 160-171, 2011.

BESKOW, S.; NORTON, D. L.; MELO, C. R. Hydrological prediction in a tropical watershed dominated by Oxisols using a distributed hydrological model. **Water Resources Management**, Reidel, v. 23, p. 341-363, 2013.

BESKOW, S. et al. Potential of the LASH model for water resources management in data-scarce basins: a case study of the Fragata River basin, Southern Brazil. **Hydrological Sciences Journal**, Oxford, v. 61, p. 2567–2578, 2016.

BEVEN, K. J.; KIRKBY, M. J. A physically based, variable contributing area model of basin hydrology. **Hydrological Sciences Bulletin**, Oxford, v. 24, p. 43-69, 1979.

BUENO, E. O. et al. Desempenho do modelo Swat para diferentes critérios de geração de unidades de resposta hidrológica. **Scientia Agraria**, Piracicaba, v. 18, 2017.

BURNASH, R. J. C. The NWS river forecast system-catchment modeling. In: Singh, V.J., (Ed.), Computer Models of Watershed Hydrology, **Water Resources Publication**, Highlands Ranch, Colorado, p. 311–366, 1995.

CALDEIRA. T. L. Aprimoramento computacional do modelo Lavras Simulation of Hydrology (LASH): aplicação em duas bacias do Rio Grande

do Sul. 2008. 120p. **Dissertação** (Mestrado em Recursos Hídricos) – Universidade Federal de Pelotas, Pelotas, 2016.

CALDEIRA. T. L. et al. LASH hydrological model: An analysis focused on spatial discretization. **Catena**, Amsterdam, v. 173, p. 183-193, 2019.

COMPANHIA ENERGÉTICA DE MINAS GERAIS; UNIVERSIDADE FEDERAL DE LAVRAS. (Brasil). **Modelo Fitográfico da Bacia do Rio Grande.** Lavras, 2018. Disponível em: < http://sig.projetoriogrande.ti.lemaf.ufla.br/>. Acesso em: 20 mar. 2019.

COLLISCHONN, W. Simulação hidrológica de grandes bacias. 2001. 194 p. **Tese** (Doutorado em Recursos Hídricos e Saneamento Ambiental) - Universidade Federal do Rio Grande do Sul, Porto Alegre, 2001.

COLLISCHONN, W. et al. Forecasting River Uruguay flow using rainfall forecasts from a regional weather-prediction model. **Journal of Hydrology**, Amsterdam, v. 305, n. 1, p. 87-98, 2005.

COLLISCHONN, W. et al. The MGB/IPH model for large-scale rainfall-runoff modeling. **Hydrological Sciences Journal**, Oxford, v. 52, n. 5, p. 878–895, 2007.

COLLISCHONN, W.; TUCCI, C. E. M. Simulação hidrológica de grandes bacias. **Revista Brasileira de Recursos Hídricos**, Porto Alegre, v. 6, n. 1, p. 95-118, 2001.

CUNGE, J. A. On The Subject Of A Flood Propagation Computation Method (Musklngum Method). **Journal of Hydraulic Research**, Delft, v. 7 n. 2 p. 205-230, 1969.

DICKINSON, R. E. Modeling evapotranspiration for the threedimensional global climate models**. Climate Processes and Climate Sensitivity**, American Geophycial Union, Washington, DC, p. 58–72, 1984.

FERNANDES FILHO, E.I.; CURI, N. **Mapa de solos do estado de Minas Gerais**. (2010). Belo Horizonte, MG: Fundação Estadual Do Meio Ambiente (FEAM).

FUKUNAGA, D.C. et al. Application of the SWAT hydrologic model to a tropical watershed at Brazil. **Catena**, v. 125, p. 206–2013, 2015.

GASSMAN, P.W. et al. The soil and water assessment tool: historical development, applications, and future research directions. **Transactions of the ASABE**, Saint Joseph, v. 50, n. 4, p. 1211–1250, 2007.

GUILHON, L.G.F.; ROCHA, V.F.; MOREIRA, J.C. Comparação de métodos de previsão de vazões naturais a aproveitamentos hidroelétricos. **Revista Brasileira de Recursos Hídricos,** Porto Alegre, v. 12, n. 3, p.13-20, 2007.

HAVRYLENKO, S.B. et al. Assessment of the soil water content in the Pampas region using SWAT. **Catena**, Amsterdam, v. 137, p. 298–309, 2016.

LIU, J.; WANG, S.; LI, D. The analysis of the impact of land-use changes on flood exposure of Wuhan in Yangtze river basin, China. **Water Resources Management**, v. 28, p. 2507–2522, 2014.

LOHMANN, D. et al. Regional scale hydrology: I., formulation of the VIC-2L model coupled to a routing model. **Hydrological Sciences Journal**, Oxford, v. 43, n. 1, p. 131-141, 1998.

MARSIK, M.; WAYLEN, P. An application of the distributed hydrologic model CASC2D to a tropical montane watershed**. Journal of Hydrology**, Amsterdam, v. 330, n. 3/4, p. 481-495, 2006.

MELLO, C. R. et al. Development and application of a simple hydrologic model simulation for a Brazilian headwater basin. **Catena**, Amsterdam, v. 75, n. 3, p. 235-247, 2008.

MELLO, C. R. et al. Sea surface temperature (SST) and rainfall erosivity in the Upper Grande River Basin, Southeast Brazil. **Ciências e Agrotecnologia**, Lavras, v. 36, n. 1, p. 53–59, 2012.

MELLO, C.R. et al. Agricultural watershed modeling: a review for hydrology and soil erosion processes. **Ciências e Agrotecnologia**, Lavras, v. 40, p. 7–25, 2016

MELLO, C.R. et al. Water balance in a neotropical forest catchment of southeastern Brazil. **Catena**, Amsterdam v. 173, p. 9-21, 2019.

MISHRA, S. K. et al. A modified SCS-CN method: characterization and testing. **Water Resources Management**, Washington, v. 17, n. 1, p. 37-68, 2003.

MISHRA, S. K.; SINGH, V. P. A relook at NEH-4 curve number data and antecedent moisture condition criteria. **Hydrological processes**, Chichester, v. 20, n. 13, p. 2755-2768, 2006.

MOTOVILOV, Y.G. et al. Validation of a distributed hydrological model against spatial observations. **Agricultural and Forest Meteorology**, v. 98–99, p. 257–277, 1999.

MORIASI, D. N. et al. Hydrologic and water quality models: performance measures and evaluation criteria. **Transactions of the ASABE**, Saint Joseph, v. 58, n. 6, p. 1763-1785, 2015.

NASH, J. E.; SUTCLIFFE, J. V. River flow forecasting through conceptual models part I: a discussion of principles. **Journal of Hydrology**, Amsterdam, v. 10, p. 282-290, 1970.

NEITSCH, S. L. et al. **Soil and water assessment tool**: theoretical documentation version 2005. Temple: Blackland Research Center, 541 p., 2005.

NEITSCH, S. L. et al. Soil and water assessment tool: theorical documentation version 2009. **Texas Water Resources Institute Technical**. Report No. 406. Texas A&M University System. September. 2011.

OLIVEIRA, V. A. et al. Land-use change impacts on the hydrology of the Upper Grande river basin, Brazil. **Cerne**, Lavras, v. 24, n. 4, p. 334–343, 2018.

OPERADOR NACIONAL DO SISTEMA ELÉTRICO. (Brasil). **Metodologia para a previsão de vazões uma semana à frente na bacia do alto/médio rio Grande**. ONS: Rio de Janeiro, 2008.

PEREIRA, D. dos R. et al. Hydrological simulation in a basin of typical tropical climate and soil using the SWAT Model Part II: Simulation of hydrological variables and soil use scenarios. **Journal of Hydrology**: Regional Studies, Amsterdam, v. 5, p. 149–163, 2016.

PINTO, L.C. et al. Role of Inceptisols in the Hydrology of Mountainous Catchments in Southeastern Brazil**. Journal of Hydrologic Engineering**, Reston, v. 21, p. 05015017, 2015.

RAWLS, W. J. et al. Infiltration and soil water movement. In: MAIDMENT, D. R. (Ed.). **Handbook of hydrology**. New York: McGraw-Hill, 1993. p. 1-51.

SCS. **National Engineering Handbook**. Soil Conservation Service/USDA, Washington. 1971

SHI, P. et al. Effects of land-use and climate change on hydrological processes in the Upstream of Huai river, China**. Water Resources Management**, Reidel, v.27, p. 1263–1278, 2013.

STACKELBERG, N. O. von et al. Simulation of the hydrologic effects of afforestation in the Tacuarembó River Basin, Uruguay. **Transactions of the ASABE**, Saint Joseph, v. 50, n. 2, p. 455-468, 2007.

TUCCI, C. E. M. **Modelos hidrológicos**. 2. ed. Porto Alegre: UFRGS, 2005. 678 p.

VAN LIEW, M.W.; ARNOLD, J.G.; GARBRECHT, J.D. Hydrologic simulation on agricultural watersheds: choosing between two models. **Transactions of the ASABE**, Saint Joseph, v. 46, p. 1539–1551, 2003.

VIOLA, M. R. Simulação hidrológica na região Alto Rio Grande a montante do reservatório de Camargos/CEMIG. 2008. 120p. **Dissertação** (Mestrado em Engenharia de Água e Solo) – Universidade Federal de Lavras, Lavras, 2008.

VIOLA, M. R. Simulação hidrológica na cabeceira da bacia hidrográfica do Rio Grande de cenários de uso do solo e mudanças climáticas A1B. 2011. 286p. **Tese** (Doutorado em Engenharia de Água e Solo) Universidade Federal de Lavras, Lavras, 2011.

VIOLA, M. R. et al. Modelagem hidrológica na bacia hidrográfica do Rio Aiuruoca, MG**. Revista Brasileira de Engenharia Agrícola e Ambiental**, Campina Grande, v.13, p.581–590, 2009.

VIOLA, M. R et al. Hydrological Modeling in a watershed of the Lower Araguaia River Basin, TO. **Journal of Biotechnology and Biodiversity**, Oxford, v.3, n. 3, p.38–47, 2012.

VIOLA, M. R. et al. Applicability of the Lash model for hydrological simulation of the Grande River Basin, Brazil. **Journal of Hydrologic Engineering**, v. 18, p. 1639–1652, 2013.

VIOLA, M. R. et al. Impacts of Land-use Changes on the Hydrology of the Grande River Basin Headwaters, Southeastern Brazil. **Water Resources Management**, Reidel, v. 28, p. 1-14, 2014. doi: 10.1007/s11269-014-0749-1.

VIOLA, M. R. et al. Assessing climate change impacts on Upper Grande River Basin hydrology, Southeastern Brazil**. International Journal of Climatology**, Chichester, v. 35, p. 1054–1068, 2015.

WIGMOSTA, M. S.; VAIL, L. W.; LETTENMAIER, D. P. A distributed hydrology-vegetation model for complex terrain. **Water Resources Research**, Washington, v. 30, n. 6, p. 1665-1679, Dec. 1994.

ZAAPA, M. Multiple-response verification of a distributed hydrological model at different spatial scales. 2002. 167 p. **Thesis** (Ph.D. in Natural Science) - Swiss Federal Institute of Technology, Zurich, 2002.

ZHANG, H. G. et al. Potential effects of climate change on runoff in the Yellow River Basin of China. **Transactions of the ASABE**, Saint Joseph, v. 50, n. 3, p. 911-918, June 2007.

ZHANG, Y. et al. Effects of plant roots on soil preferential pathways and soil matrix in forest ecosystems. **J. Forest. Res**. v.26, p. 397-404, 2015.

ZHOU, M. C. et al. Estimating potential evapotranspiration using Shuttle worth Wallace model and NOAA-AVHRR NDVI data to feed a distributed hydrological model over the Mekong River basin. **Journal of Hydrology**, Amsterdam, v. 327, n. 1/2, p. 151-173, 2006.

ARTIGO 2 - CLIMATE CHANGE PROJECTIONS OF THE HYDROPOWER GENERATION IN FURNAS HYDROPOWER PLANT, SOUTHEAST BRAZIL

ABSTRACT: Approximately 70% of all the electric energy produced in Brazil comes from hydropower plants (HPs), what has become the country dependent on the hydrological regime. In the context of hydropower generation, the Grande River Basin (GRB) can be highlighted, being responsible for 8.7% of the electric energy produced in Brazil. Some studies have been carried out to investigate the impacts from the weather in water resources and consequently in hydropower production. This study aims to simulate the changes in the hydrology and in the potential hydropower generation of the GRB delineated from the Furnas Hydropower Plant (FHP) (GRB-FHP), which is the main facility of Southeastern Brazil. The LASH model was applied to study the hydrological impacts in the GRB defined upstream from FHP (GRB-FHP). This model was forced by the Regional Climate Models (RCM) Eta-HadGEM-ES, Eta-MIROC5 and Eta-CanESM2 for the period between 2007 and 2099, taking into account the Representative Concentration Pathways (RCPs) 4.5 and 8.5. The mean annual hydropower production was estimated by means of Power Duration Curves (PDC), considering as reference the installed capacity and the average and minimum hydropower produced over time by the FHP. LASH was able to simulate the monthly runoff in the GRB-FHP for the baseline period (1961-2005). A significant reduction in the monthly streamflow, for both RCPs, was observed throughout the XXI Century, demonstrating that changes in the hydrology of the basin may take place in FHP. Reductions of up to 53% in the hydropower generation are expected to occur at the end of the Century.

KEYWORDS: Hydrologic simulation, Regional Climate Models, Hydroelectricity, climate change.

1. INTRODUCTION

The water resources availability is directly related to the surface features, the climate and the water uses. In a watershed, hydrological processes are driven by changes in the climate, which are influenced by human actions in both short and long terms. These changes can harm the environment, the economy, and society. In this sense, the developing countries are the most vulnerable to climate change (LUBINI; ADAMOWSKI, 2013; MELLO et al., 2008; VIOLA et al., 2015).

In 1998, the World Meteorological Organization (WMO) and the United Nations Environment Programme (UNEP) jointly created the Intergovernmental Panel of the Climate Change (IPCC) to drive the scientific studies related with climate change impacts and propose possible mitigations and adaption (IPCC, 2013). The most common approach to assess climate change impacts is to verify changes in the rainfall and temperature patterns. Both climate variables impact the runoff regime of the basins since rainfall is directly related to the streamflow generation and the temperature to the evapotranspiration (JIANG et al., 2004; TAN et al., 2017).

The main tools used to project climate scenarios are the Global Climate Models (GCM). Their outputs have been widely applied to study the impacts on the hydrology caused by the changes on the climate (HO; THOMPSON; BRIERLEY, 2016; KOPYTKOVSKIY; GEZA; MCCRAY, 2015; OUYANG et al., 2015). However, these models do not have a finer spatial resolution to meet the runoff studies in the watershed scale. Thus, the GCMs are coupled with regional climate models (RCM) for downscaling the outputs (CHOU et al., 2014a). In this sense, local and regional effects on the climate, mainly the orographic effects, are further detailed, which allows assessing accurate simulations from hydrological models.

Approximately 70% of all electric energy produced in Brazil comes from hydropower plants, which means that the country is very susceptible to impact from climate change. This impact is clearer during the dry season of

the hydrological years, which affects the generation capacity of the facilities as their reservoirs depend on the rainfall events in the rainy season for water storage. Changes in the rainy season can threaten the reservoirs' operation, compromising the hydropower generation. Besides, the increase on temperatures affect the evaporation rates from the reservoirs and the basin, increasing the vulnerability of the hydropower system (BUENO et al., 2017; OLIVEIRA et al., 2017; VIOLA et al., 2015).

Grande river is one of the most important tributaries of the Parana river basin, which is the most important tributary of the La Plata River Basin. The Grande River Basin (GRB) is located in Southeastern Brazil, with headwaters in the Mantiqueira range region (bordering the States of São Paulo and Minas Gerais). This basin is very relevant in the context of the Brazilian hydropower generation system. There is a cascade of 14 hydropower plants installed directly in the Grande River, being some of the reservoirs for water accumulation (NÓBREGA et al., 2011; VIOLA et al., 2014). GRB has a total installed power capacity of approximately 7,600 MW, which accounts for 8.7% of the hydropower generation in Brazil. Therefore, changes in the climate might potentially impact both the hydrology of the basin and hydropower production capacity of center-south Brazil.

Furnas Hydropower Plant (FHP) is located in the middle GRB, Southeastern Brazil. It was built in the 1950s and began working in September/1963. FHP has 1,312 MW of installed capacity. Besides, the FHP reservoir has an important hydrological function, which is the streamflow regulation of the Grande river. Thus, this facility is strategic for the Brazilian hydropower systems. Other ten downstream plants are sustained by the regulated streamflow from FHP, increasing the efficiency of the Brazilian hydropower system (FURNAS, 2007). Therefore, FHP plays a fundamental role in the Brazilian National Interconnected System (SIN) since the majority of the electric energy produced by the facilities of the SIN is derived from the hydropower plants (ONS, 2017).

Some hydrological studies have been carried out in the GRB due to its relevant hydropower capacity. Viola et al. (2015) studied the impacts of the climate changes on the hydrology in the Upper Grande River Basin. They assessed the impacts with the LASH hydrological model forced with outputs of the Eta-HadCM3 RCM and the premises of the A1B scenario. Oliveira et al. (2017) assessed the impacts on both hydrology and hydropower generation of three plants (Camargos, Itutinga, and Funil). These authors highlighted that together these facilities are important to maintain the hydropower production and contribute to the FHP reservoir. They found that Camargos, Itutinga, and Funil might stop working at 28%, 69% and 50% of the time until the end of the century, respectively.

Other similar studies have been conducted in Brazil. Siqueira Júnior, Tomasella and Rodriguez (2015) appraised the impacts of climate change on the hydropower generation in the Madeira river basin, Amazon region, throughout the XXI Century, using eight GCMs. They concluded that there is not a clear trend between the GCMs. Some of them showed reduction up 45% of the hydropower generation, whereas other GCMs pointed increases up 38% from 2071 to 2099. Globally, Van Vliet et al. (2016) evaluated climate change impacts on the hydro and thermoelectricity generation. They used five GCMs and the Representative Concentration Pathways (RCP) 2.5 and 8.5 Wm^{-2}. The results indicated that the greatest part of the hydropower plants (61% to RCP 2.5 and 74% to RCP 8.5) are in regions where the projections showed significant reductions on the streamflow. This might result in global reductions in the useful capacity of these facilities.

Because of the relevance of GRB and FHP for the Brazilian Hydropower System, the objective of this study was to: (i) model the hydrology of the GRB-FHP; and (ii) assess the impacts of climate change on the hydropower plant generation capacity up to the end of Century. In order to reach these purposes, the Lavras Simulation of Hydrology (LASH) model was calibrated and validated to simulate the naturalized streamflow in the FHP. Afterwards, the LASH model was forced by the outputs of the RCM

Eta-HadGEM2-ES, Eta-MIROC5 and Eta-CanESM2, working with the RCPs 4.5 and 8.5 to simulate the hydrological projections and their impacts on the hydropower capacity generation of FHP.

2. MATERIAL AND METHODS

2.1 Study area

This study was developed in the GRB upstream from Furnas Hydropower Plant (GRB-FHP), Southeast Brazil, accounting for an area of 52,000 km². Its location is presented in Figure 1. The available water in the GRB is fundamental for the country since the Grande river supplies 65 municipalities and 14 hydropower plants installed directly along its course. FHP reservoir is the largest one and is responsible for the hydrological regulation of the entire GRB aiming to maintain water at a constant level in the downstream reservoirs.

Overall, there are two Köppen climate types in the studied basin, Cwa and Cwb, both with dry and cool winters and rainy and hot summers, thus the hydrological year is well defined from October of a year to September in the following year (VIOLA et al., 2014). The mean maximum and minimum temperatures are, respectively, 22^{o}C and 8^{o}C, and the mean annual precipitation is approximately 1,500 mm (MELLO et al., 2012).

Figure 1 – Geographical location of the Grande River Basin and Furnas Hydropower Plant in the Brazilian territory, and the river stage and rain gauges and meteorological stations.

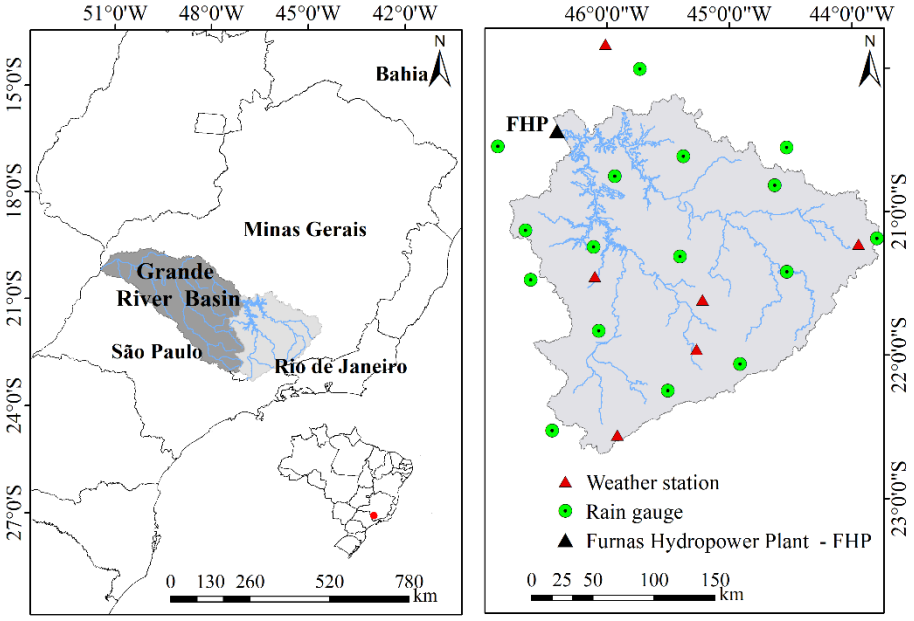

Source: From author (2019).

2.2 The Lavras Simulation of Hydrology model (LASH)

The LASH model was developed to simulate streamflows in data-scarce basins (Mello et al. 2008). Since its first version, LASH has been constantly improved by implementing automatic calibration, improving the spatial distribution by both cells and sub-watersheds and more recently, using hydrological response units (HRU). This model has been applied in different geomorphological contexts in Brazil with good accuracy (BESKOW et al., 2011; BESKOW; NORTON; MELLO, 2011, 2013; CALDEIRA et al., 2019; MELLO et al., 2008; VIOLA et al., 2014).

LASH is a semi-conceptual, deterministic, long-term model. It is structured based on three reservoirs: the direct surface runoff (D_{SUP}), which is based on the modified CN method (MISHRA et al., 2003); and sub-surface runoff (D_{SS}); and baseflow (D_B) reservoirs, which are based on the Brooks and

Corey equation (RAWLS et al., 1993) for porous mean (NOVÁK; HLAVÁCIKOVÁ, 2019). LASH model converts the surface runoff components into discharge considering linear reservoirs in each sub-basin, taking the time lag of the fluxes. Routing streamflow in the channels is made by Muskingum-Cunge linear method (CUNGE, 1969) and evapotranspiration according to means of the Penman-Monteith equation (ALLEN et al., 1998) considering the vegetative cover (aerodynamic and stomatal conductance) and restriction by soil moisture (VIOLA et al., 2013).

The simulations are carried out through water balance in a soil layer determined following the dominant land-use in each sub-watershed. It was defined 69 sub-watersheds (and respective HRUs) in GRB-Furnas, identifying 21 different combinations of HRUs, following the land-use, slope and soils classes in Table 1. LASH model was previously calibrated in a daily time step and then accounted into monthly time step.

Table 1 – Soil, vegetation and slope classes used to structure the HRUs in GRB-Furnas.

Soil	**Slope (%)**	**Vegetation**
Latosol – Bw	0 – 10	Atlantic Forest
Argisol – Bt	10 - 20	Cerrado
Cambisol – Bi	>20	Pasture
Litholic Neosol – Ne	-	Agriculture
Rock - R	-	-

Source: From author (2019).

2.3 Basic maps and hydrological and climatological datasets

The climate datasets used for calibration and validation in LASH model were obtained in the “Hydrological Information System" (HidroWeb) from the "National Water Agency" (ANA), and "National Institute of Meteorology" (INMET/BDMEP) (FIGURE 1). The weather variables assessed were the daily values of maximum and minimum temperatures, income solar radiation, relative humidity and wind speed, which were used to

calculate the evapotranspiration according to the Penman-Monteith equation (ALLEN et al., 1998).

The streamflow data used for the hydrological model calibration and validation were obtained through the “Operador Nacional do Sistema Elétrico" (ONS). These data are naturalized by the ONS, which means that the streamflow that would be observed in the river without any anthropogenic activities, such as reservoir operation upstream and withdrawal of water by human or irrigation consumption (GUILHON; ROCHA; MOREIRA, 2007). These datasets are calculated based on a rebuilding process that applied 96 stochastic models to predict the daily streamflow in each hydropower plant of the SIN (MÜLLER; RIZZI; FILL, 2011). Such data are reliable as backgrounds for planning the hydropower plants in short and middle terms (ONS, 2008).

LASH model requires maps of soils and land-uses (FIGURES 2a and 2b). The land-use map was developed based on LANDSAT-8 images of 2018 (CEMIG; UFLA, 2018). The uses are pasture (40.76%), native forests (25.07%), agriculture (18.17%), Brazilian savanna - Cerrado (9.88%), water bodies (2.57%), and eucalyptus (2.45%) and others less pronounced, such as urban areas (0.91%) e bare soils (0.19%).

Soil map was adapted from the Minas Gerais State Environmental Foundation (FEAM, 2010) in a scale of 1:650,000. The dominant classes are Latosols (42.96%), Argisols (25.76%), Cambisols (23.08%), and Litholic Neosol (3.27%) and others less highlighted that account 4.93%.

Figure 2 – Land-use map (a) and soil map (b) of the Grande River Basin upstream from Furnas Hydropower Plant.

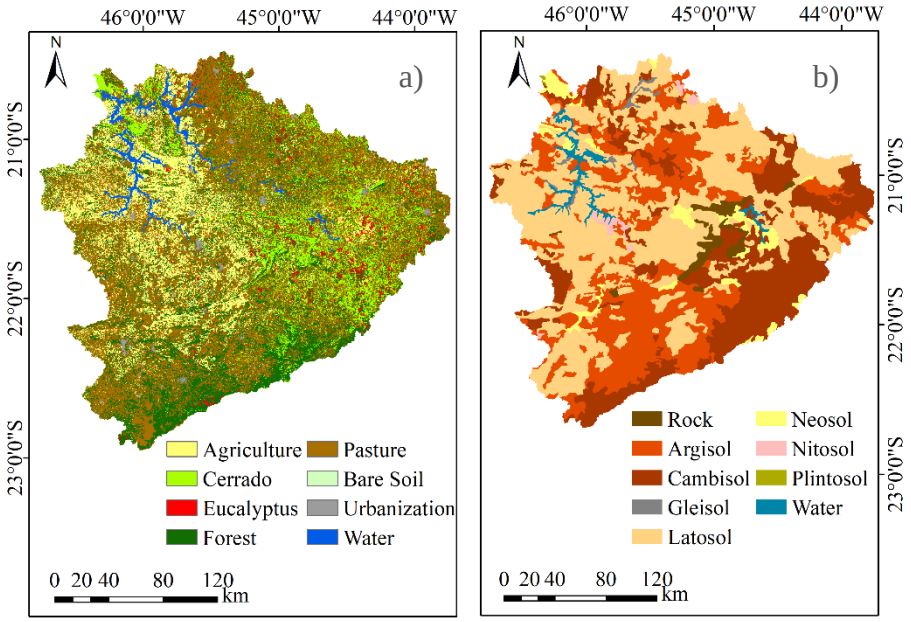

Source: from author (2019).

2.4 Calibration and validation of the LASH model

The naturalized streamflows downstream FHP were obtained from 1990 to 2007. The LASH model was calibrated for the period between 1990 and 2000 and validated in the period from 2001 to 2007. For the model's warmup, the years of 1990 and 2001 were used, respectively, for the calibration and validation phases.

In this version of the LASH model has been calibrated 5 parameters, which are the initial abstraction coefficient (λ), hydraulic conductivity of the sub-surface reservoir (K_{SS}; mm day^{-1}), hydraulic conductivity of the groundwater reservoir (KB; mm day^{-1}); a routing parameter for superficial reservoir (C_{SUP}), and a routing parameter for the sub-surface reservoir (C_{SS}) (BESKOW; NORTON; MELLO, 2011; MELLO et al., 2008; VIOLA et al., 2014). For this purpose, it was applied the manual calibration procedure using

the Nash-Sutcliffe coefficient (NASH; SUTCLIFFE, 1970) as the objective function.

The model performance was evaluated based on the Nash-Sutcliffe coefficient (C_{NS}) (NASH; SUTCLIFFE, 1970), the log(C_{NS}) coefficient (NASH; SUTCLIFFE, 1970), and the percentage ratio between observed and calculated volumes ((Δ_V) (COLLISCHONN, 2001).

2.5 Climate change projections

The potential impacts on the streamflow to FHP were estimated based on the hydrological simulations. LASH model was forced by climate projections from the Global Circulation Models (GCM) MIROC5, HadGEM2-ES and CanESM2. The outputs from the GCMs were dynamically downscaled by the Eta/CPTEC model (BLACK, 1994; MESINGER et al., 1988). Details about the GCM used in this study can be found in Watanabe et al. (2010), Oliveira et al. (2017), Collins et al. (2011) and Martin et al. (2011). Thus, the projections from the Regional Circulation Models (RCM) were generated by CPTEC/INPE and made available on the PROJETA Platform to the baseline period (1961-2005) and throughout the XXI Century, divided into three time slice (2007-2040; 2041-2070; 2071-2099), using the RCPs 4.5 and 8.5, with 20-km spatial resolution (CHOU et al., 2014a,b; LYRA et al., 2017). The weather variables used to assess the hydrological impacts were precipitation, maximum and minimum temperatures, income solar radiation, relative humidity, and wind speed.

The procedure used for simulation of the hydrological impacts was adapted from Cousino, Becker and Zmijewski (2015) and Oliveira et al. (2019). The RCMs outputs for the baseline and the RCPs 4.5 and 8.5 were obtained in a grid box, taking the nearest grid point of each one of the 15 rain-gauges and 6 meteorological stations applied to calibrate the LASH model (FIGURE 3).

Figure 3 – Grid points of the Regional Climate Models nearest of the rain gauges and meteorological stations used in this study.

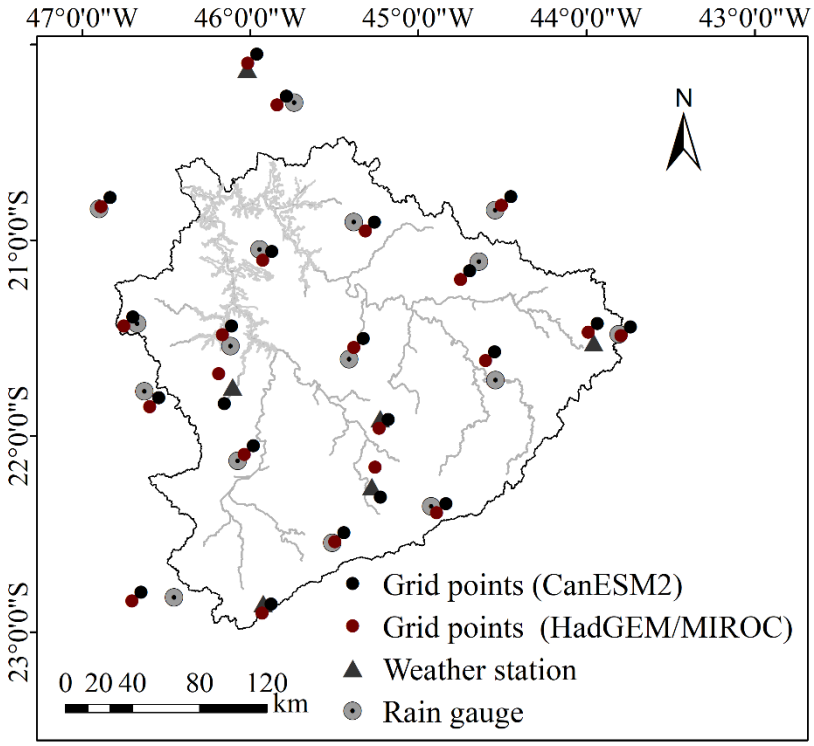

Source: From author (2019).

Nevertheless, the weather variables from the RCMs may present systematic errors due to the numerical solution procedures of the models, being necessary to remove them before forcing the hydrological model (BERG; FELDMANN; PANITZ, 2012; GRAHAM; ANDRÉASSON; CARLSSON, 2007; SHRESTHA; ACHARYA; SHRESTHA, 2017; TEUTSCHBEIN; SEIBERT, 2012). The correction of these systematic errors was implemented fitting a linear regression between the mean monthly observed and projected weather variables to the baseline (SHRESTHA; ACHARYA; SHRESTHA, 2017). This procedure can be described by the following equations:

$$V^{*}_{contr}(d) = V_{contr}(d)\left[\frac{\mu_m(V_{obs}(d))}{\mu_m(V_{contr}(d))}\right] \quad (1)$$

$$V^{*}_{scen}(d) = V_{scen}(d)\left[\frac{\mu_m(V_{obs}(d))}{\mu_m(V_{contr}(d))}\right] \quad (2)$$

$$T^{*}_{contr}(d) = T_{contr}(d) + \mu_m(T_{obs}(d)) - \mu_m(T_{contr}(d)) \quad (3)$$

$$T^{*}_{scen}(d) = T_{scen}(d) + \mu_m(T_{obs}(d)) - \mu_m(T_{contr}(d)) \quad (4)$$

Where V(d) and T(d) are the daily weather variables (precipitation, income solar radiation, relative air moisture, and wind speed) and daily temperature, respectively; μm is the monthly average value of the variable; and "contr", "scen" and "obs" are the baseline, scenarios and observed data, respectively. Values of V(d) and T(d) < 1 indicate that the projections are overestimating the observed data; > 1 indicate that they are underestimating the observed data. Afterwards, the monthly streamflow simulations of the times slices were compared with the baseline (1961-2005), assessing the hydrological impacts.

2.6 Assessment of the projected climate change on the hydropower generation

The impacts of the climate change on the hydropower generation were estimated following the methodology proposed by Mohor et al. (2015). FHP presents an installed capacity of 1,312 MW, average head fall of 91 m, average reservoir depth of 15 m, and average flooded area of 1,209 km^2 (ANA, 2017; ONS, 2017). The potential hydropower is defined as the maximum power capacity that may be used considering the facility efficient, streamflow and head fall:

$$N_P = Q * H * \rho_w * g * \eta \quad (5)$$

Where N_P is the potential power (W); Q is the discharge ($m^3\ s^{-1}$); H is the nominal fall (m); ρ_w is the water bulk density ($kg\ m^{-3}$); g is the gravitational force ($m\ s^{-2}$), and η is the plant efficiency 80% (OLIVEIRA et al., 2017; SAMPAIO; RAMOS; SAMPAIO, 2005).

Using equation 5 and the streamflow simulated to the baseline and projections, by the LASH model, it was possible to estimate the FHP potential hydropower. The baseline and projected potential hydropower values were converted into power duration curves (PDCs). A PDC is a graphic that indicates the maximum hydropower estimated over time (VOGEL; FENESSEY, 1995). The impacts on the hydropower generation were estimated comparing the PDCs calculated for the baseline and future times periods, considering both the installed and minimum power.

Similar to the flow duration curves, the PDC is a graphic representation of the percent of time that a given hydropower potential was equaled or exceeded and are mainly used for studies of hydropower feasibility. It illustrates the relationship between the frequency and magnitude of the hydropower potential. The integration of the area below the PDC constrained by the installed and minimum capacities represents the hypothetical average annual energy production, in MWh/year (VOGEL; FENESSEY, 1995).

The monthly hydropower values produced in FHP between 2002 and 2016 were obtained in the National Electric Energy Agency (ANEEL). In this period, the minimum hydropower was 26 MW, observed in June/2015, and the installed and average hydropower values were 1,312 MW and 531 MW, respectively. These reference values were used to evaluate the hydropower feasibility considering the climate change projections throughout the century.

3. RESULTS AND DISCUSSION

3.1 Calibration and validation of the LASH model

The calibration of LASH model for the GRB-FHP was carried out according to a monthly time step. Table 2 shows the precision statistics used to evaluate the performance of the model in calibration and validation.

Table 2 – Monthly precision statistics for the calibration and validation of the LASH model to the Grande River Basin upstream from Furnas Hydropower Plant.

Application	Statistics		
	C_{NS}	Log (C_{NS})	Δ_V (%)
Calibration	0.89	0.86	2.19
Validation	0.85	0.83	11.52

Source: From author (2019).

LASH model was able to adequately simulate the naturalized streamflows from FHP since the C_{NS} values for calibration and validation were greater than 0.80, allowing to classify the hydrological model as "very good" (MORIASI et al., 2015). Also, LASH showed a great performance in simulating the recession limbs of the hydrograph, (log (C_{NS}) > 0.8).

The observed and calculated volumes ratio (Δv – TABLE 2) is an index that shows the model's capability in the evapotranspiration estimates (COLLISCHONN, 2001). A slight overestimation of the evapotranspiration was observed, especially in the validation phase. However, these values can be considered low and non-significant for the water balance. Collischonn (2001) obtained Δv values between -5% and 6% simulating the streamflows in the Taquari-Antas basin, South Brazil, using the MGB-IPH model. Viola et al. (2014) obtained ΔV values between -10% and 13% for basins in the Upper Grande River Basin region, using a previous version of LASH model. These values of ΔV strength the LASH model capability to simulate the water balance in the studied basin.

Figure 4 depicts the observed and simulated hydrographs and respective hyetographs. We can observe the good accuracy of the LASH model, with great adherence between the estimated and observed streamflows, including the peak and baseflow ones, in both calibration and validation phases.

Figure 4 – Observed and simulated monthly streamflows and hyetographs at Furnas Hydropower Plant in the calibration and validation phases.

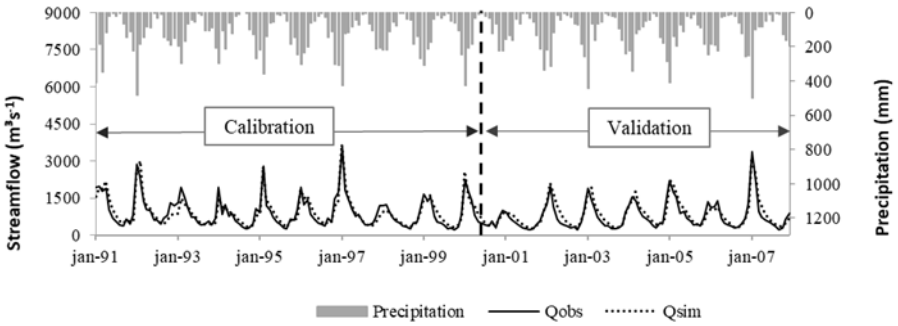

Source: From author (2019).

In Brazil, related studies have used naturalized streamflows for calibration of hydrological models in hydropower plants (FOY et al., 2015; MATHEUSSEN et al., 2000; NOBREGA et al., 2011; OLIVEIRA et al., 2017; WEEDON et al., 2015). Oliveira et al. (2017) used monthly naturalized streamflows for calibration of SWAT model to assess the climate change impacts on hydropower generation of three facilities in the Upper Grande river basin. They found satisfactory results a monthly time step (C_{NS} ranging from 0.53 to 0.74). Nobrega et al. (2011) calibrated MGB-IPH model with the same purpose to 10 hydropower plants in GRB. They obtained C_{NS} and log (C_{NS}) ranging from 0.85 to 0.95, and ΔV values smaller than 0.05% in calibration and 7% in the validation phase, similar to LASH model simulations in GRB-FHP. In these studies, the hydrologic models were classified as "good".

3.2 Climate projections in the GRB-FHP

The average of the weather variables projected by the RCMs (precipitation, minimum and maximum temperatures, income solar radiation, wind speed, and relative humidity), after the removal of the systematic errors, are presented in Table 3.

Table 3 – Average of the weather variables projected by the RCMs (annual precipitation – P; minimum and maximum temperatures – Tmax and Tmin; income solar radiation – Rad; wind speed – Vv; relative air moisture content – UR) to Grande River Basin upstream from Furnas Hydropower Plant under the RCPs 4.5 and 8.5.

Eta-HadGEM2-ES							
	Period	P	Tmax	Tmin	Rad	Vv	UR
		mm	°C		MJ m^{-2} dia^{-1}	m s^{-1}	%
Baseline	1961 - 2005	1452	26.2	13.8	16.7	1.35	77.3
RCP 4.5	2007-2040	996	29.0	14.1	17.2	1.40	67.5
	2041-2070	1164	29.6	15.2	17.3	1.39	69.8
	2071-2099	1182	30.3	15.8	17.3	1.39	69.6
RCP 8.5	2007-2040	1074	29.5	14.5	17.6	1.44	67.0
	2041-2070	1107	31.1	16.1	17.8	1.44	66.6
	2071-2099	947	34.1	18.2	18.0	1.48	61.4
Eta-MIROC5							
	Period	P	Tmax	Tmin	Rad	Vv	UR
		mm	°C		MJ m^{-2} dia^{-1}	m s^{-1}	%
Baseline	1961 - 2005	1452	26.2	13.8	16.7	1.35	77.4
RCP 4.5	2007-2040	1385	27.0	14.7	16.2	1.34	76.8
	2041-2070	1492	27.6	15.4	16.4	1.33	77.7
	2071-2099	1326	28.2	15.7	16.4	1.33	76.2
RCP 8.5	2007-2040	1282	27.2	14.8	16.3	1.32	75.8
	2041-2070	1480	28.3	16.0	16.4	1.33	76.9
	2071-2099	1521	29.6	17.3	16.4	1.32	77.9
Eta-CanESM2							
	Period	P	Tmax	Tmin	Rad	Vv	UR
		mm	°C		MJ m^{-2} dia^{-1}	m s^{-1}	%
Baseline	1961 - 2005	1457	26.3	13.9	16.8	1.38	77.2
RCP 4.5	2007-2040	1419	28.1	15.4	17.1	1.40	73.5
	2041-2070	1300	29.6	16.4	17.4	1.40	69.6

	2071-2099	1333	30.2	17.0	17.0	1.39	68.8
RCP 8.5	2007-2040	1391	28.2	15.5	17.1	1.39	73.4
	2041-2070	1202	31.0	17.1	17.7	1.40	65.8
	2071-2099	934	34.9	19.2	18.4	1.49	54.2

Source: From author (2019).

We can observe that the rainfall projections indicated a significant reduction in the mean annual precipitation throughout XXI Century. The most severe reductions were found when deriving information from Eta-CanESM2 and Eta-HadGEM2-ES, with values of -35.9% and -34.8%, respectively, for the RCP 8.5. Based on the Eta-MIROC5 projections, the average precipitation reduction was lower and may reach 8.7% in relation to the baseline (1961-2005) in the RCP4.5. For RCP8.5, this value may be reduced by 4.8% in the end of Century (2071-2099).

Regarding the average maximum and minimum temperatures, in all time slice and RCPs and RCMs, the results showed an increase in both variables. Eta-HadGEM2-ES projected an average increase of 4.1 and 2.0^{o}C, respectively, to maximum and minimum temperatures in RCP 4.5. For RCP 8.5, this RCM projected an average increase of 7.9°C and 4.4^{o}C, respectively. On the other hand, Eta-MIROC5 projected lower increases, being 2.0^{o}C and 1.9^{o}C, respectively, to maximum and minimum temperatures in RCP 4.5, and 3.0^{o}C and 4.0^{o}C, respectively, in RCP 8.5. Eta-CanESM2 simulated significant increases, however, different from the other RCMs. These increases were more relevant to maximum than minimum temperatures, being 9.0^{o}C and 5.0^{o}C in RCP8.5, respectively. Eta-HadGEM2-ES and Eta-CanESM2 projected greater warming than Eta-MIROC5 throughout XXI Century. Chou et al. (2014a) reported that Eta-HadGEM2-ES projections were more sensitive than Eta-MIROC5 to the increasing greenhouse emissions in their projections using both RCM for South America.

In addition to temperature behavior, relative humidity projected by Eta-CanESM2 and Eta-HadGEM2-ES, on average, was reduced in

comparison to the baseline, by up to 29.7% and 16,5%, respectively. Thus, increases on temperature, reduction on precipitation and relative humidity might lead to an increase in evapotranspiration, then, reducing the water availability to runoff generation.

3.3 Streamflow projections in GRB-FHP

The average observed and simulated monthly streamflow for baseline and times slices are presented in Figure 5. From December to August, the streamflows were overestimated in relation to the baseline, when LASH was forced with Eta-HadGEM2-ES. However, when it was forced with Eta-MIROC5 and Eta-CanESM2, the streamflows were underestimated between September and March and overestimated from April to August in relation to the baseline. Overall, the Eta-HadGEM2-ES, Eta-MIROC5 and Eta-CanESM2 produced average errors of, respectively, 17%, 20%, and 19%.

These errors were similar to those obtained by Viola et al. (2015), using LASH forced with Eta-HadCM3 (A1B SRES scenario and 40 km spatial resolution) in the Upper Grande river basin. They reported average errors of 21.6%, 12%, 25%, and 29% for Aiuruoca, Grande (delineated in headwater region), Sapucai and Verde basins, respectively. The simulation presented in our study showed a greater accuracy than Viola et al. (2015) study. Possible explanations for this are the improvements made in the LASH structure, especially the implementation of the HRUs along with climate data with better spatial resolution (20 km).

Figure 5 – Average observed and projected monthly streamflows simulations from Eta-HadGEM2-ES, Eta-MIROC5 and Eta- CanESM2 to Grande River Basin upstream from Furnas Hydropower Plant.

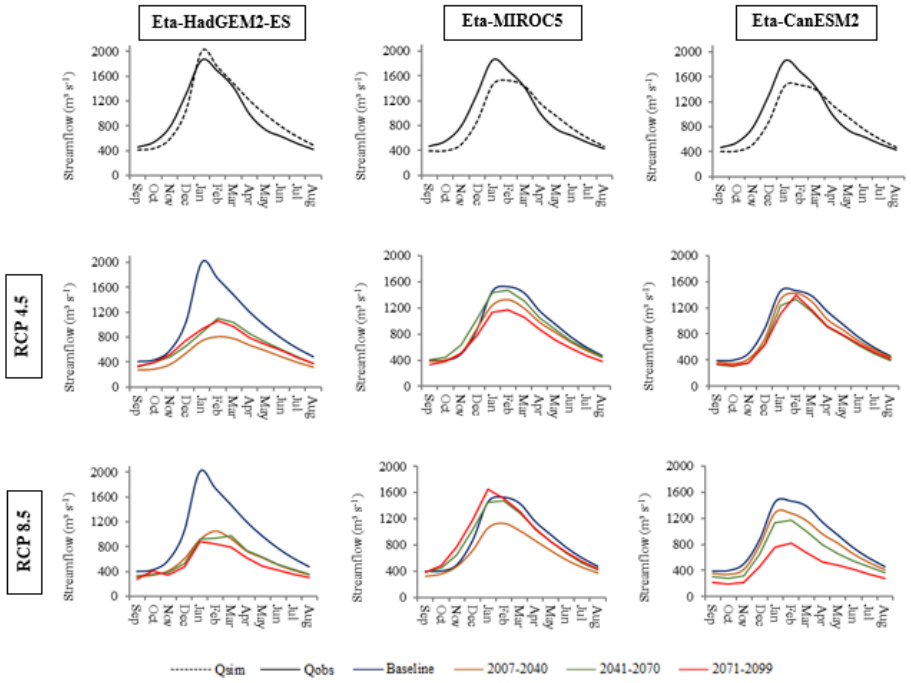

Source: From author (2019).

Using SWAT model forced with Eta-HadGEM2-ES and Eta-MIROC5 RCMs, Oliveira et al. (2017) simulated the streamflows from Camargos, Itutinga, and Funil hydropower plants in Upper Grande river basin. Comparing to the baseline, they obtained average errors of 37%, 21.2% and 7.6% when Eta-HadGEM2-ES was applied, respectively. Greater errors were obtained with Eta-MIROC5, being 41%, 24.4%, and 8.2%, respectively. Thus, except for Funil Hydropower Plant, the results obtained to FHP were considerably superior, which was linked with the quality of the respective calibration of the hydrological models.

Errors between simulated and observed monthly streamflows are expected. Such errors occur due to the use of the RCMs as inputs in the hydrological models, which may not be able to reproduce accurately the

streamflow behavior, with deviations in both magnitude and time. The physical structure of the RCMs, their parametrizations, downscaling technique, and the RCPs are the main sources of uncertainties, leading to differences between observed and simulated streamflows (AMORIM; CHAFFE, 2019; OLIVEIRA; PEDROLLO; CASTRO, 2015; PRUDHOMME; DAVIES, 2009).

Uncertainties regarding the calibration of hydrological models may induce differences between observed and simulated discharges. In the study of Oliveira et al. (2017) and the present study for FHP, both hydrological models were calibrated using the naturalized streamflows. These values consist of estimations made by stochastic models and assumptions required by them, which can generate errors in the hydrology of the basin. Importantly, these datasets are the only source of streamflow data for simulation purposes and have been used for forecasting in the long term.

Assessing Figure 6, the results indicate that the average monthly streamflows simulated by LASH forced with the RCMs projections might be significantly reduced throughout the XXI Century. Projections using Eta-HadGEM2-ES showed the greatest reductions in streamflows in relation to the baseline, mainly in the rainy season (December to April), in the first time slice (2007-2040) for RCP4.5. In this period, streamflows might be reduced up to 63% (January). However, at the end of the second (2041-2070) and third (2071-2099) times slices, the results showed slight increases concerning the first time slice. Based on RCP8.5, it was observed reductions in streamflows up to 56% in January at the end of Century (compared to the baseline).

Considering Eta-MIROC5, decreases in streamflows were also observed, however, in a different manner concerning the other RCMs. In RCP4.5, the greatest decreases were observed in the third time slice (2071-2099) (up to 26% for March). Based on RCP 8.5, the greatest decreases were observed in the first time slice (up to 29% for May). This RCM was the only one that projected a small increase in average monthly streamflows. These

projections were observed for the period from October to December throughout the Century in both RCPs.

The Eta-CanESM2 in the RCP4.5 presented similar behavior to Eta-MIROC5, with less marked decreases in streamflow if compared to the Eta-HadGEM2-ES. The greatest decreases were projected for the second and third time slice, reaching 30% in November. On the other hand, considering the RCP8.5, the projected decreases were more highlighted and similar to the ones projected by Eta-HadGEM2-ES. It was observed consecutive reductions throughout the Century, especially in the third time slice and for November (57%).

The streamflows projected in this study are similar to those obtained by Oliveira et al. (2017) for the Upper Grande River basin. Overall, the results suggest significant decreases in the monthly streamflows in the 21st Century. The most severe changes were projected by the Eta-HadGEM2-ES. Decreases in the streamflows in a region with a marked dry season might lead to severe and prolonged droughts, harming the water resources. Our results showed that there is a considerable probability of reduction on the water availability in the GRB-FHP throughout 21st Century. This trend is explained by the decrease in the precipitation amount and increase in evapotranspiration both projected by the RCMs, which would reduce the surplus water for runoff. Thus, this behavior of water balance might compromise the hydropower generation as well as the functioning of the Brazilian interconnected system, since FHP is strategic for maintaining the operation of this system.

3.4 Projections of the changes in the hydropower generation capacity of FHP

The climate change projections on the hydropower generation of FHP were evaluated by means of power-duration-frequency curves (PDF) (VOGEL; FENESSEY, 1995). For this purpose, the hydropower generation was estimated as a function of the hydrological impacts from climate change,

comparing it with the facility installed capacity and average and minimum hydropower generation from 2001 to 2016. Respectively, these values are 1,312 MW, 531 MW and 26 MW (ANEEL, 2017).

Figure 6 depicts the PDFs built to FHP based on the monthly streamflows simulated by LASH forced with the RCMs to the baseline. The simulated PDFs present adequate agreement with the observed ones. The C_{NS} values calculated based on the PDFs simulated and observed were 0.98, 0.94, and 0.95, respectively, to Eta-HadGEM2-ES, Eta-MIROC5 and Eta-CanESM2. These values demonstrate the great accuracy of the PDFs simulated based on the LASH model.

Figure 6 – Power-duration-frequency curves (PDF) derived from monthly simulated and observed streamflows to the baseline – 1961 a 2005 (a. Eta-HadGEM2-ES; b. Eta-MIROC5; c. Eta-CanESM2).

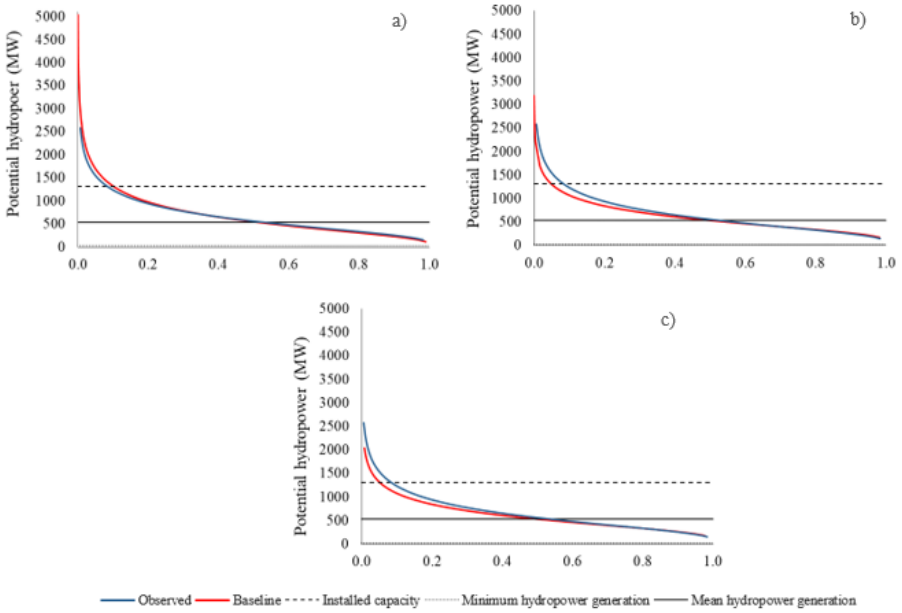

Source: From author (2019).

The PDF obtained based on Eta-HadGEM2-ES projections showed greater accuracy, however, presenting a slight overestimation for the lower frequencies (the greatest power values). For the interval with the minimum

and average hydropower, this PDF showed a great agreement with the observed PDF (FIGURE 6a).

The PDFs simulated based on Eta-MIROC5 projections were similar to the ones obtained from Eta-CanESM2 and both were different from Eta-HadGEM2-ES for the baseline period. These PDFs showed a slight underestimation trend for the hydropower values associated with the lower frequencies. For the minimum and the average hydropower interval, these PDFs showed greater similarity with the observed PDF (FIGURE 6b,c).

Taking the installed hydropower in FHP (1,312 MW) and the observed PDF, this value can be assured in 8% of the time. Using the simulated PDFs, it was obtained 10.2%, 4.9% and 5.1% of the time, respectively, by the Eta-HadGEM2-ES, Eta-MIROC5, and Eta-CanEMS2-ES. Considering the average hydropower (531 MW), the facility was able to assure this value in 53% of the time, whereas based on the simulated PDFs, it was 51.2%, 50%, and 48.8%, respectively, by Eta-HadGEM2-ES, Eta-MIROC5, and Eta-CanEMS2-ES. The minimum hydropower (26 MW) was assured in 100% of the time in all the PDFs (observed and simulated). Thus, these results strength that the PDF based on the Eta-HadGEM2-ES had greater performance.

The simulated PDFs to the baseline and times slices are presented in Figure 7. It is also presented the exceeding times associated with the installed and the average and minimum hydropower generation of the FHP. The exceeding time associated with minimum hydropower observed in FHP (26 MW) is 100%. This value is the most critical observed in this facility, and according to the projections, it will not be observed again up the end of the XXI Century. Further analyzing Figure 7, the most severe projections are found to Eta-HadGEM2-ES and RCP8.5. The exceeding time to the average hydropower might be reduced from 51.2% in the baseline to 13.8% in 2071-2099 time slice, whereas to the RCP4.5, it might be 28.7%. Taking as reference the installed hydropower in FHP, the exceeding time might be

reduced from 10.2% in the baseline to only 1% and 1.2% at the end of Century to the RCPs 8.5 and 4.5, respectively.

Figure 7 – Power-duration-frequency curves (PDCs) for the baseline (1961-2005) and times slices (2007-2040; 2041-2070; and 2071-2099), and the exceeding times simulated from Power Duration Curves (PDC), by LASH, forced with the RCMs (Eta-HadGEM2-ES, Eta-MIROC5 and Eta-CanESM2) in the RCP4.5 and 8.5.

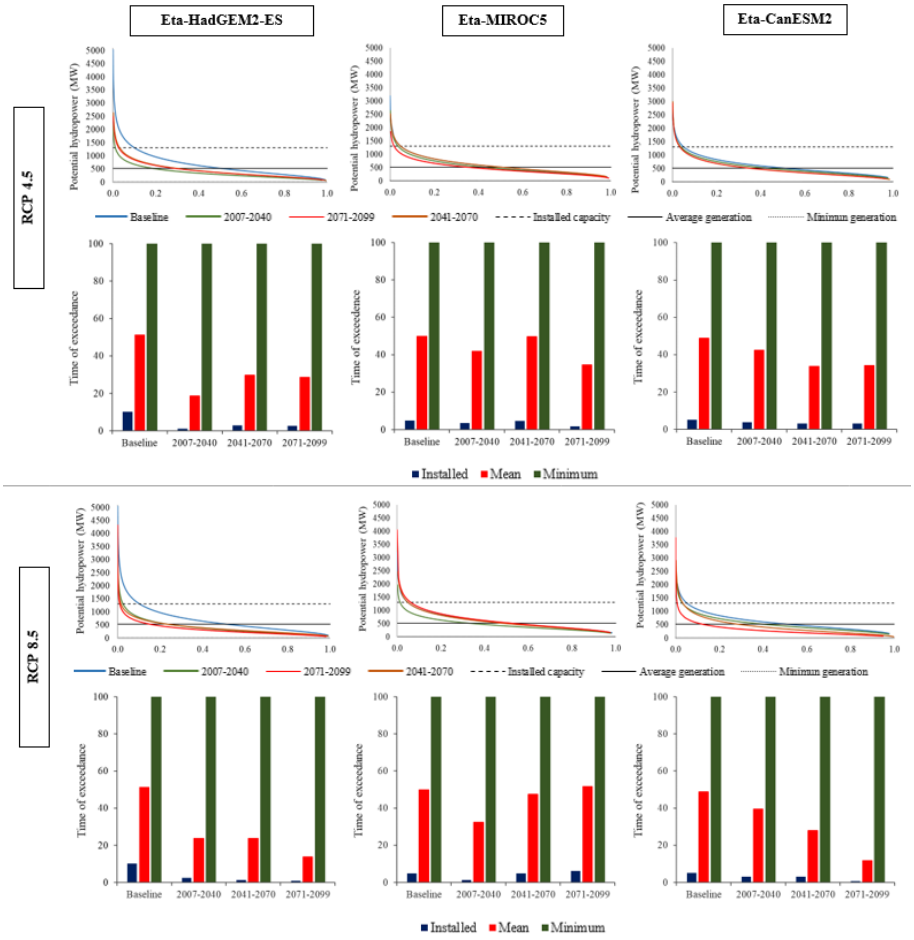

Source: From author (2019).

Regarding the projections from Eta-MIROC5, the results indicate that the most severe projection of the installed hydropower is expected in the first time slice (2007-2040) with reductions in the exceeding time from 4.9% to

1.3% and 1.8%, respectively to RCP 4.5 and 8.5. Considering the average hydropower, the reduction might be from 50% to 32.5% and 34.7%, respectively, to RCP4.5 and 8.5.

Assessing the Eta-CanESM2 projections, the greatest change was projected to 2071-2099 time slice and RCP8.5. Decreases in the installed and average hydropower might be changed from 5.1% to 0.7% and from 48.8% to 11.7%, respectively. Taking the RCP 4.5 projections, these decreases might be from 5.1% to 3.3% and from 48.8% to 33.8%, respectively.

Oliveira et al. (2017) assessed the impacts of climate change in the potential hydropower generation in the Camargos, Itutinga and Funil facilities in the Upper Grande river basin (upstream FHP). They applied the Eta-HadGEM2-ES and Eta-MIROC5 RCMs and RCPs 4.5 and 8.5 throughout 21st Century and observed that the former RCM projected that these facilities might shut down in 27.7%, 69.1% and 50% of the time, respectively. However, projections using the Eta-MIROC5, Funil hydropower plant might not be operating in 5.3% of the time, while for Camargos Hydropower Plant, the minimum generation will be assured in the 21st Century.

Mohor et al. (2015) assessed the climate change impacts in the potential hydropower generation in the Teles Pires Hydropower Plant, Tapajós river basin, Amazon region. The authors embedded eight RCMs in the MDH-INPE hydrological model, and the results pointed that in the most critical projection, this facility might shut down in 59% of the time between 2041 and 2070 because the minimum hydropower capacity might not be reached.

In Table 5, it is presented the percentage differences of the annual hydropower generation projected by the RCMs in relation the baseline to FHP. The Eta-HadGEM2-ES and Eta-CanEMS2 projections indicated that the most critical situation is expected to the end of the 21st Century and RCP8.5. Eta-HadGEM2-ES projected decreases of 45.6% in the annual hydropower in the last time slice, whereas Eta-CanEMS2 projected decreases of 53%. On the other hand, Eta-MIROC5 also projected decreases on the annual hydropower,

however, these decreases were much less critical, being 14.6% and 16.7% in the RCP4.5 (third time slice) and 8.5 (first time slice), respectively.

Table 5 – Percentage changes in the potential annual hydropower generation in FHP simulated by the LASH forced with the RCMs and RCPs 4.5 and 8.5.

Annual potential hydropower generation (x10^6 MWh/year)				
Projections/RCM		Eta-HadGEM2-ES	Eta-MIROC5	Eta-CanEMS2-ES
	Baseline	4.7	4.9	4.8
RCP 4.5	2007-2040	-34.9%	-8.5%	-8.3%
	2041-2070	-22.6%	-0.2%	-19.0%
	2071-2099	-23.9%	-14.6%	-20.6%
RCP 8.5	2007-2040	-33.6%	-16.7%	-10.8%
	2041-2070	-29.7%	-3.8%	-27.7%
	2071-2099	-45.6%	2.1%	-53.0%

Source: From author (2019).

Mohor et al. (2015) obtained a decrease of 82% in the annual hydropower generation in Teles Pires plant in the RCP 8.5. Galvão and Braga (2015) verified anomalous behavior in the Annual Affluent Natural Energy (ANE) using Eta-HadGEM2-ES and Eta-MIROC5. The RCMs and RCPs for all times slices showed a decrease in ANE in Southeast Brazil, where it is located FHP. The greatest anomaly was observed with Eta-HadGEM2-ES and RCP8.5, with a decrease of 45% in the 2071-2099 time slice. Using Eta-MIROC5 and RCP8.5, the greatest decrease was 20% in the 2011-2040 time slice. We can see that there was a significant difference between the RCMs, which is related to the downscaling uncertainties, scenarios emission, and hydrological modeling.

In the study of Oliveira et al. (2017), the simulations based on the Eta-HadGEM2-ES projections showed a decrease in the annual potential

hydropower generation of -57.2%, -66.1% and -38.2% in Camargos, Itutinga, and Funil plants, respectively, between 2071-2099. Eta-MIROC5 projections might generate reductions, however, in lower levels, as obtained to FHP in this study. Hasan and Wyseure (2018) applied the SWAT model to assess the climate change impacts on the hydropower generation from a plant in the Jubones river basin, Ecuador. They observed that this facility might be affected by a decrease of 13.14% in its hydropower production mainly in the dry season in relation to the baseline.

The results of this study suggest a plausible decrease on the hydropower generation at FHP. This decrease can affect the Brazilian Electric Energy System since FHP is the most important facility of GRB. Thus, the energy production might be serious harmed throughout the Century. Besides, FHP is the most important reservoir of Southeast Brazil, which means it has a relevant impact on the hydrology of GRB. The water storage in this reservoir can be seriously affected by the changes in the climate throughout the 21st Century, increasing the conflicts for water in the GRB (MINAS GERAIS, 2014).

Several elements can affect the hydropower generation such as economic activities demand, unexpected and planned interruptions, energy supply, among others. In the face of a scarcity water scenario, which is plausible in the near future, the Brazilian government has been forced to produce a greater amount of electric energy from other sources, mainly through thermic plants. These plants use mineral coal as fuel, which is more expensive and releases a greater amount of greenhouse gas to the atmosphere, feeding global warming (COELHO et al., 2016).

4. CONCLUSIONS

In this study, the climate change impacts on the hydrological behavior of the GRB-FHP and on the hydropower generation of FHP, Southeast Brazil, were assessed. LASH model was able to simulate the naturalized streamflows

from FHP, producing reliable results when forced by the RCMs Eta-HadGEM2-ES, Eta-MIROC5, and Eta-CanEMS2 under the conditions of the RCPs 4.5 and 8.5.

The RCMs projections showed that important changes on the climate of the GRB-FHP might occur throughout the 21st Century, negatively impacting the streamflows for the FHP. Overall, the RCMs projected a significant decrease in precipitation as well as a significant increase in evapotranspiration, which lead to a decrease in water surplus for streamflow in GRB.

Hydrological projections from the Eta-HadGEM2-ES demonstrated the greatest reduction in the annual streamflows throughout the XXI Century, which might compromise the water resources available in the basin. Under the RCP4.5, these projections were more significant in the first time slice (2007-2040), whereas for RCP8.5 in third time slice (2071-2099).

Using the Eta-MIROC5, decreases in the streamflows are concentrated in third time slice and RCP4.5, while for the RCP8.5, the projections showed greater decreases in the first time slice. Eta-CanESM2 in RCP4.5 projected similar trend to Eta-MIROC5, showing decreases less pronounced when compared to Eta-HadGEM2-ES. However, under RCP8.5, the decreases on the streamflows were closer to those from Eta-HadGEM2-ES.

Due to the projected decrease in streamflow, the hydropower generation at FHP can be deeply impacted, with trends of decrease throughout the 21st Century. The most severe projections for the average hydropower generation were: i) Eta-HadGEM2-ES, RCP 8.5 for third time slice, with decreases in the exceeding time from 51.2% to 13.8% to average hydropower generation; ii) Eta-CanESM2, RCP 8.5 and third time slices, with decreases from 48.8% to 11.7%.

Regarding the annual potential hydropower generation, the most severe decreases were projected to the end of the XXI Century and RCP8.5 with the Eta-HadGEM2-ES and Eta-CanESM2-ES, being, respectively,

46.6% and 53%. Eta-MIROC5 also projected decreases in the annual hydropower generation, however, less severe (14.6% and 16.7%, respectively, for RCP 4.5 in the third time slice and 8.5 in the first time slice).

REFERENCES

AGÊNCIA NACIONAL DE ENERGIA ELÉTRICA. (Brasil). **Banco de Informações de Geração** - BIG. Brasília, 2017. Disponível em: <http://www 2.aneel.gov.br/aplicacoes/ capacidadebrasil/capacidadebrasil.cfm>. Acesso em: 20 jan. 2019.

ALLEN, R.G. et al. Grop evapotranspiration: guidelines for computing crop water requirements. **Irrigation and Drainage**. Paper No. 56, FAO, Italy, 1998. 328p.

AMORIM, P.B.; CHAFFE, P.B. Towards a comprehensive characterization of evidence in synthesis assessments: the climate change impacts on the Brazilian water resources. **Climate Change**, Dordrecht, v. 36, n. 1, p. 53–59, 2012.

BLACK, T. L. The New NMC Mesoscale Eta Model: Description and Forecast Examples. **Weather and Forecasting**, v. 9, n. 2, p. 265-278, 1994.

BERG, P.; FELDMANN, H.; PANITZ, H. J. Bias correction of high resolution regional climate model data. **Journal of Hydrology**, Amsterdam, v. 448, p. 80-92, 2012.

BESKOW, S.; MELLO, C. R.; NORTON, L. D. Development, sensitivity and uncertainty analysis of LASH model. **Scientia Agricola**, Piracicaba, v. 68, n. 3, p. 265-393, 2011.

BESKOW, S. et al. Performance of a distributed semi-conceptual hydrological model under tropical watershed conditions. **Catena**, Amsterdam, v. 86, n. 3, p. 160-171, 2011.

BESKOW, S.; NORTON, D. L.; MELLO, C. R. Hydrological prediction in a tropical watershed dominated by Oxisols using a distributed hydrological model. **Water Resources Management**, Reidel, v. 23, p. 341-363, 2013.

BUENO, E. O. et al. Desempenho do modelo Swat para diferentes critérios de geração de unidades de resposta hidrológica. **Scientia Agraria,** Piracicaba, v. 18, p.114-125, 2017.

CALDEIRA. T. L. et al. LASH hydrological model: An analysis focused on spatial discretization. **Catena**, Amsterdam, v. 173, p. 183-193, 2019.

CHOU, S. C. et al. Assessment of Climate Change over South America under RCP 4.5 and 8.5 Downscaling Scenarios. **American Journal of Climate Change**, Bethesda, v. 3, p. 512-525, 2014a.

CHOU, S.C. et al. Evaluation of the Eta Simulations Nested in Three Global Climate Models. **American Journal of Climate Change**, Bethesda, v. 3, n. 5, p. 438-454, 2014b.

COELHO, C.A.S. et al. The 2014 southeast Brazil austral summer drought: regional scale mechanisms and teleconnections. **Climate Dynamics**, Berlin, v. 46, n. 11, p. 3737–3752, 2016.

COLLINS, W.J. et al. Development and evaluation of an Earth-System model – HadGEM2. **Geoscientific Model Development**, v. 4, n. 4, p. 1051–1075, 2011.

COLLISCHONN, W. et al. Forecasting River Uruguay flow using rainfall forecasts from a regional weather-prediction model. **Journal of Hydrology**, Amsterdam, v. 305, n. 1-4, p. 87–98, 2005.

COMPANHIA ENERGÉTICA DE MINAS GERAIS; UNIVERSIDADE FEDERAL DE LAVRAS. (Brasil). **Modelo Fitográfico da Bacia do Rio Grande**. Lavras, 2018. Disponível em: < http://sig.projetoriogrande.ti.lemaf.ufla.br/>. Acesso em: 20 mar. 2019.

COUSINO, L. K; BECKER, R. H.; ZMIJEWSKI, K. A. Modeling the effects of climate change on water, sediment, and nutrient yields from the Maumee River watershed. **Journal of Hydrology**: Regional Studies, Amsterdam, v. 4, p. 762-775, 2015.

CUNGE, J. A. On The Subject Of A Flood Propagation Computation Method (Musklngum Method). **Journal of Hydraulic Research**, Delft, v. 7 n. 2 p. 205-230, 1969.

DUAN, Q., SOROOSHIAN, S., GUPTA, V. 1992. Effective and Efficient Global Optimization for Conceptual Rainfall-Runoff Models. **Water Resources Research,** Ann Abor, v. 28, n. 4, p. 1015-1031, 1992.

FERNANDES FILHO, E.I.; CURI, N**. Mapa de solos do estado de Minas Gerais**. (2010). Belo Horizonte, MG: Fundação Estadual Do Meio Ambiente (FEAM).

FOY, C. et al. Multisite Assessment of Hydrologic Processes in Snow-Dominated Mountainous River Basins in Colorado Using a Watershed Model**. Journal of Hydrologic Engineering**, Reston, v. 20, n.10, 2015.

FURNAS. 1957-1967 – Como tudo começou. **Revista FURNAS**. Ed. especial, n. 337, fev. 2007. 17 p. Disponível em: <http://www.furnas.com.br/arqtrab/ddppg/revistaonline/linhadireta/rf337_57-67.pdf>. Acesso em: 15 mai. 2019.

GALVÃO, C.O.; BRAGA, C.F. **Brasil 2040**: Documento síntese: Resumo executivo. Brasília: PRESIDÊNCIA DA REPÚBLICA; SECRETARIA DE ASSUNTOS ESTRATÉGICOS, 2015. 58 p. Disponível em: http://www.mma.gov.br/images/arquivo/80182/BRASIL-2040-Resumo-Executivo.pdf. Acesso em: 15 abr. 2019.

GRAHAM, L.P.; ANDRÉASSON, J.; CARLSSON, B. Assessing climate change impacts on hydrology from an ensemble of regional climate models, model scales and linking methods – a case study on the Lule River basin. **Climatic Change**, Dordrecht, v.81 (S1), p. 293–307, 2007.

GUILHON, L.G.F.; ROCHA, V.F.; MOREIRA, J.C. Comparação de métodos de previsão de vazões naturais a aproveitamentos hidroelétricos. **Revista Brasileira de Recursos Hídricos,** Porto Alegre, v. 12, n. 3, p.13-20, 2007.

HASAN, M.M.; WYSEURE, G. Impact of climate change on hydropower generation in Rio Jubones Basin, Ecuador. **Water Science and Engineering**, v. 11, n. 2, p. 157–166, 2018.

INTERGOVERNMENTAL PANEL ON CLIMATE CHANGE. **Climate Change 2013**: The Physical Science Basis. Working Group I Contribution to the Fifth Assessment Report of the IPCC. Cambridge: Cambridge University, 2013.

JIANG, T. et al. Review on Regional Water Resources Assessment Models under Stationary and Changing Climate. **Water Resources Management**, Washington, v. 18, p. 591-612, 2004.

KOPYTKOVSKIY, M.; GEZA, M.; MCCRAY, J. E. Climate-change impacts on water resources and hydropower potential in the Upper Colorado River Basin. **Journal of Hydrology**, Amsterdam, v.3, p. 473-493, 2015.

LYRA, A. et al. Climate change projections over three metropolitan regions in Southeast Brazil using the non-hydrostatic Eta regional climate model at 5-km resolution. **Theoretical and Applied Climatology**. v. 132, p. 663-682, 2017.

LUBINI, A.; ADAMOWSKI, J. Assessing the Potential Impacts of Four Climate Change Scenarios on the Discharge of the Simiyu River, Tanzania Using the SWAT Model. **International Journal of Water Sciences**, v.2, n.1, p. 1–12, 2013.

MARTIN, G.M. et al. The HadGEM2 family of Met Office Unified Model climate configurations. **Geoscientific Model Development**, Munich, v. 4, n.3, p. 723–757, 2011. doi: 10.5194/gmd-4-723-2011.

MATHEUSSEN, B. et al. Efects of land cover change on streamflow in the interior Columbia River Basin (USA and Canada). **Hydrological Processes**, Chichester, v. 14, n. 5, p. 867-885, 2000.

MELLO, C. R. et al. Development and application of a simple hydrologic model simulation for a Brazilian headwater basin. **Catena,** Amsterdam, v. 75, n. 3, p. 235-247, 2008.

MESINGER, F. A blocking technique for representation of mountains in atmospheric models. **Rivista di Meteorologia Aeronautica**, v. 44, n. 1-4, p. 195-202, 1984.

MINAS GERAIS**. Plano Diretor de Recursos Hídricos e Enquadramento de Corpos de Água da Bacia Hidrográfica do Alto Rio Grande - GD1**. Governo do Estado de Minas Gerais: Belo Horizonte, 2014. 280 p.

MISHRA, S. K. et al. A modified SCS-CN method: characterization and testing. **Water Resources Management**, Washington, v. 17, n. 1, p. 37-68, 2003.

MOHOR, G. S. et al. Exploratory analyses for the assessment of climate change impacts on the energy production in an Amazon run-of-river hydropower plant. **Journal of Hydrology**: Regional Studies, Amsterdam, v. 4, p. 41-59, 2015.

MORIASI, D. N. et al. Hydrologic and water quality models: performance measures and evaluation criteria. **Transactions of the ASABE**, Saint Joseph, v. 58, n. 6, p. 1763-1785, 2015.

MÜLLER, I.I.; RIZZI, N.E.; FILL, H.D. Avaliação da vazão indisponibilizada por usinas hidrelétricas em bacias hidrográficas e a cobrança pelo uso da água no setor elétrico. **Floresta**, Curitiba, v. 41, n. 4, p. 737–750, 2011.

NASH, J. E.; SUTCLIFFE, J. V. River flow forecasting through conceptual models part I: a discussion of principles. **Journal of Hydrology**, Amsterdam, v. 10, p. 282-290, 1970.

NÓBREGA, M. T. et al. Uncertainty in climate change impacts on water resources in the Rio Grande Basin, Brazil. **Hydrology and Earth System Sciences**, Saskatoon, v. 15, p. 585-595, 2011.

NOVÁK, V.; HLAVÁCIKOVÁ, H. **Applied Soil Hydrology**. 2. ed. Porto Alegre: Springer, 2019.

OLIVEIRA, G. G.; PEDROLLO, O. C.; CASTRO, N. M. R. As incertezas associadas às condições climáticas obtidas pelo modelo ETA CPTEC/HADCM3: Avaliação comparativa entre os dados simulados e observados de precipitação, evapotranspiração e vazão na bacia hidrográfica do rio Ijuí, Brasil. **Revista Brasileira de Meteorologia**, São José dos Campos, v.30, 101 - 121, 2015.

OLIVEIRA, V. A. et al. Modeling the effects of climate change on hydrology and sediment load in a headwater basin in the Brazilian Cerrado biome**. Ecological Engineering**, v. 133, p. 20-31, 2019.

OLIVEIRA, V. A. et al. Assessment of climate change impacts on streamflow and hydropower potential in the headwater region of the Grande river basin, Southeastern Brazil. **International Journal of Climatology**, Chichester, v. 37, p. 5005-5023, 2017.

OPERADOR NACIONAL DO SISTEMA ELÉTRICO. (Brasil). **Metodologia para a previsão de vazões uma semana à frente na bacia do alto/médio rio Grande**. ONS: Rio de Janeiro, 2008.

OPERADOR NACIONAL DO SISTEMA ELÉTRICO. **O Sistema Interligado Nacional - SIN**. 2017. Disponível em: <http://ons.org.br/pt/paginas/sobre-osin/o-que-e-o-sin>. Acesso em: 15 dez. 2017.

OUYANG, F. et al. Impacts of climate change under CMIP5 RCP scenarios on streamflow in the Huangnizhuang catchment. Stochastic **Environmental Research and Risk Assessment**, Berlin, v. 29, p. 1781-1795, 2015.

PRUDHOMME, C.; DAVIES, H. Assessing uncertainties in climate change impact analyses on the river flow regimes in the UK. Part 2: future climate. **Climatic Change**, Dordrecht, v. 93, n. 1-2, p. 197-222, 2009.

SAMPAIO, L.M.B.; RAMOS, F.S.; SAMPAIO, Y. Privatização e eficiência das usinas hidrelétricas brasileiras. **Economia Aplicada**, Ribeirão Preto, v.9, n. 3, p. 465-480, 2005.

SIQUEIRA JÚNIOR, J.L.; TOMASELLA, J.; RODRIGUEZ, D.A. Impacts of future climatic and land cover changes on the hydrological regime of the Madeira River basin. **Climatic Change**, Dordrecht, v. 129 n. 1-2, p.117–129, 2015.

SHRESTHA, M.; ACHARYA, S. C.; SHRESTHA, P.K. Bias correction of climate models for hydrological modelling – are simple methods still useful?. **Meteorological Applications**, 2017.

TAN, M. L. et al. Climate change impacts under CMIP5 RCP scenarios on water resources of the Kelantan River Basin, Malaysia. **Atmospheric Research**, Amsterdam, v. 189, p. 1-10, 2017.

TEUTSCHBEIN, C.; SEIBERT, J. Bias correction of regional climate model simulations for hydrological climate-change impact studies: Review and evaluation of different methods. **Journal of Hydrology**. Amsterdam, v. 456, p. 12-29, 2012.

TUCCI, C. E. M. **Modelos hidrológicos**. 2. ed. Porto Alegre: UFRGS, 2005. 678 p.

VAN VLIET, M.T.H. et al. Power-generation system vulnerability and adaptation to changes in climate and water resources. **Nature Climate Change**, v. 6, n. 4, p. 375-381, 2016.

VIOLA, M. R. et al. Applicability of the Lash model for hydrological simulation of the Grande River Basin, Brazil. **Journal of Hydrologic Engineering**, Reston, v. 18, p. 1639–1652, 2013.

VIOLA, M. R. et al. Impacts of Land-use Changes on the Hydrology of the Grande River Basin Headwaters, Southeastern Brazil. **Water Resources Management**, Washington, v. 28, p. 1-14, 2014.

VIOLA, M. R. et al. Assessing climate change impacts on Upper Grande River basin hydrology, Southeast Brazil. **International Journal of Climatology**, Chichester, v. 35, n. 6, p. 1054-1068, 2015.

VOGEL, R. M.; FENESSEY, N. M. Flow–duration curves II: review of applications in water resources planning. **Water Resour**. Bull., v. 31, n. 6, p. 1029–1039, 1995.

WATANABE, M. et al. Improved Climate Simulation by MIROC5: Mean States, Variability, and Climate Sensitivity. **Journal of Climate**, Boston, v. 23 n. 23, p. 6312-6335, 2010.

WEEDON, G. P. et al. Evaluating the Performance of Hydrological Models via Cross-Spectral Analysis: Case Study of the Thames Basin, United Kingdom. **Journal of Hydrometeorology,** v. 16, n. 1, p. 214-231, 2015.